



## Bio-functional electrospun nanomaterials: From topology design to biological applications

Jinpeng Han<sup>a</sup>, Likun Xiong<sup>a</sup>, Xingyu Jiang<sup>b</sup>, Xiaoyan Yuan<sup>c,\*</sup>, Yong Zhao<sup>d,\*</sup>, Dayong Yang<sup>a,\*</sup>

<sup>a</sup> School of Chemical Engineering and Technology, Key Laboratory of Systems Bioengineering (Ministry of Education), Collaborative Innovation Center of Chemical Science and Engineering (Tianjin), Tianjin University, Tianjin, 300072, PR China

<sup>b</sup> Beijing Engineering Research Center for BioNanotechnology and CAS Key Laboratory for Biological Effects of Nanomaterials and Nanosafety, CAS Center for Excellence in Nanoscience, National Center for NanoScience and Technology, Beijing, 100190, PR China

<sup>c</sup> School of Materials Science and Engineering, Tianjin Key Laboratory of Composite and Functional Materials, Tianjin University, Tianjin, 300072, PR China

<sup>d</sup> Key Laboratory of Bio-inspired Smart Interfacial Science and Technology of Ministry of Education, School of Chemistry, Beihang University, Beijing, 100191, PR China



### ARTICLE INFO

#### Article history:

Received 27 September 2018

Received in revised form 3 January 2019

Accepted 13 February 2019

Available online 16 February 2019

#### Keywords:

Electrospinning

Tissue

Engineering

Wound healing

Drug delivery

Diagnosis

### ABSTRACT

Electrospinning is a highly versatile technology to process polymers or related materials into fibrous materials with diameters ranging from micrometer to nanometer scale. In the early years, the electrospun materials were mainly polymers and the morphologies were mainly fibers. Considerable progress has been achieved in the preceding two decades, which include electrospinning of metals, metal oxides, carbon species and organic/inorganic composites, and generating more morphologies beyond fibers such as beads, tubes and even hierarchical structures. In addition, a myriad of promising applications have been explored, mainly including biological, energy, catalysis, environment and mechanical enhancement, more than half focused on biological applications.

Electrospun nanomaterials can be designed to mimic the structural features of an extracellular matrix for cell growth and nutrients transport. Such materials may be designed to enhance aesthetic wound healing, owing to the ability to absorb excess exudates, maintain a moist microenvironment to enhance epithelial regrowth, and offer painless to removal. Electrospun nanomaterials encapsulated or with attached bioactive molecules and drugs are regarded as suitable candidates for delivery applications. They may also be utilized in medical diagnosis to enhance the specificity, sensitivity and signaling capabilities due to the high porosity and large surface area. In addition, electrospun nanomaterials can be assembled into a variety of fascinating biomimic structures and functions. All these attributes make electrospinning a powerful tool for fabricating bio-functional nanomaterials for a range of biological applications concerning human health that mainly include tissue engineering, wound healing, drug/bioactive molecules delivery, diagnosis, and biomimetics.

This review highlights recent advances in the topological design and biological applications of electro-spun bio-functional nanomaterials. The topologies are categorized to portray a comprehensive “topology periodic table”, providing a concise and clear map offering a reference for scientists or engineers to opt for specific topology with desirable functions targeting a special application, as well as corresponding fabrication strategy. The topologies of electrospun nanomaterials are classified into three categories: *Individuals*, *Hybrids* and *Assemblies* according to the intrinsic logical relationships. The state-of-the-art progress on electrospun nanomaterials together with biological applications, challenges, and future directions are comprehensively summarized.

© 2019 Elsevier B.V. All rights reserved.

**Abbreviations:** Ag<sub>2</sub>S, silver sulfide; AIDS, acquired immune deficiency syndrome; DOX, doxorubicin; DRG, dorsal root ganglion; E-spin, electrospinning; ECMs, extracellular matrices; FAs, F-actin; Fe<sub>3</sub>O<sub>4</sub>, ferroferric oxide; FSP1, fibroblastic phenotype; H<sub>2</sub>S, sulfuretted hydrogen; HCl, hydrochloric acid; hMSCs, human mesenchymal stem cells; IMC, indometacin; *M. luteus*, *micrococcus luteus*; MOFs, metal-organic frameworks; NCO, isocyanate; NO, nitric oxide; NPs-in-NFs, nanoparticles-in-nanofibers; PAN, polyacrylonitrile; PbS, lead sulfide; PC, polycarbonate; PCL, poly(ε-caprolactone); PCL-PLGA, poly(ε-caprolactone)-poly(DL-lactide-co-glycolide); PDGF, platelet-derived growth factor; PECLL, poly(ethylene glycol)-b-poly(L-lactide-co-ε-caprolactone); PEO, poly(ethylene oxide); PGA, poly(glycolic acid); PHB, polyhydroxybutyrate; PLA, poly(L-lactic acid); PMMA, poly(methyl methacrylate); PS, polystyrene; PVA, polyvinyl alcohol; PVP, poly(vinyl pyrrolidone); RBCs, red blood cells; SiO<sub>2</sub>, silicon dioxide; SIRT, stress-induced rolling technology; TEPC, track-etched polycarbonate; TiO<sub>2</sub>, titanium dioxide; VEGF, vascular endothelial growth factor; VSMCs, vascular smooth muscle cells; ZrO<sub>2</sub>, zirconia; α-SMAs, α-smooth muscle actin.

\* Corresponding author.

E-mail addresses: [yuanxy@tju.edu.cn](mailto:yuanxy@tju.edu.cn) (X. Yuan), [zhaoyong@buaa.edu.cn](mailto:zhaoyong@buaa.edu.cn) (Y. Zhao), [dayong.yang@tju.edu.cn](mailto:dayong.yang@tju.edu.cn) (D. Yang).

<https://doi.org/10.1016/j.progpolymsci.2019.02.006>

0079-6700/© 2019 Elsevier B.V. All rights reserved.

## Contents

1. Introduction .....	2
2. Topological design of e-spin nanomaterials .....	2
2.1. Individuals .....	3
2.1.1. Bead, beaded fiber and fiber .....	3
2.1.2. Hollow, core-shell and multichannel .....	3
2.1.3. Porous and microcage .....	5
2.2. Hybrids .....	5
2.2.1. Nanoparticles, nanoneedles and beads .....	5
2.2.2. Drugs, bioactive molecules and cells .....	7
2.3. Assemblies .....	8
2.3.1. Nonwoven and aligned array .....	8
2.3.2. Helical and crimping .....	10
2.3.3. Patterning/complex patterning .....	10
2.3.4. Rope and tube .....	12
3. Biological applications .....	12
3.1. Tissue engineering .....	13
3.2. Wound healing .....	16
3.3. Drug/bioactive molecules delivery .....	17
3.4. Diagnosis .....	18
3.5. Biomimetics .....	21
4. Conclusion and outlook .....	22
Acknowledgements .....	22
References .....	22

## 1. Introduction

The concept of the “right” size between nanomaterials/nanotechnology and bio-systems proposed by George Whitesides [1], was subsequently implemented, followed by the explosive development of nanobiotechnology. A variety of nanotechnologies have been developed, and numerous nanomaterials have been prepared, aiming to solve practical problems or elucidate fundamental questions in biological fields [2–7]. Among those nanotechnologies and nanomaterials, electrospinning (abbreviated as ‘e-spin’) may be the most simple and straightforward technique to produce diverse biofunctional nanomaterials, adaptable to wide biological applications [4,8–12].

The term electrospinning is derived from a combination of electrostatic and spinning. In comparison with traditional spinning technologies, such as solution spinning and melt spinning in fiber science [13–18], e-spin uses electrostatic force to process polymeric solution and produce materials at micro- or nano- scale [19]. Remarkably, e-spin not only can be used to fabricate nanofibers, but also possesses the capability to versatilely manufacture nanomaterials with a myriad of topologies, from beads and hollow fibers to hierarchical structures [20]. The process of e-spin was originally patented by Gooley in 1902; afterwards, in 1969 Taylor proposed the theoretical modeling of e-spin [21,22]. However, the astonishing capability to fabricate nanomaterials was not realized until the mid-1990s [23]. Later, driven by the growing wave of nanotechnology, e-spin was reinvented as a versatile nanotechnology to prepare nanomaterials [19,20,24–28], and consequently a skyrocketing numbers of publications emerged in recent years (Fig. 1A).

The rapid development of e-spin is attributed to its overwhelming advantages: 1) the set-up is simple and inexpensive: the key instrument is a high voltage generator, and almost every lab can build their own home-made set-up; 2) the process is straightforward and rapid: just apply high voltage on polymer or polymeric composite solution; 3) the most attractive merit is the diversity of the products: almost all materials can be processed and almost all topologies can be achieved. Absolutely, the sustainable development of any technologies or materials follows the general rules: being able to solve practical problems. The flourishing development of e-spin is undoubtedly attributed to the capability of catering for a wide range of real-world applications such as energy, health

and environment [29–31]. The application fields of e-spin nanomaterials are summarized and categorized (Fig. 1B), and more than half portion is in biological subject. Five major subgroups are further classified in biological fields, including tissue engineering, wound healing, drug/bioactive molecules delivery, diagnosis and biomimetics [5,32–39].

There are already numerous excellent reviews regarding the advances of e-spin [5,12,19,22,25,26,30,39–43], and the recent advances in topological design and biological applications of electrospun nanomaterials are not comprehensively summarized yet. In this review, we don’t intend to provide the exhaustive accounts of literatures, but rather categorize the topologies and portray a “topology periodic table” comprehensively, providing a concise and clear map offering a reference for scientists or engineers to opt for specific topology with desirable functions targeting a special application, as well as corresponding fabrication strategy. We further discuss the recent progress of biological applications, demonstrating the versatility of e-spin nanomaterials.

## 2. Topological design of e-spin nanomaterials

Taking full advantage of the versatility of e-spin, a variety of fascinating topologies were fabricated by designing different spinnerets or collectors, and tuning the composition of polymer solution, e-spin parameters and environmental variables, as well as conducting post-treatments [20]. By summarizing and analyzing the current topologies and fabrication strategies of e-spin nanomaterials, a “topology periodic table” of e-spin nanomaterials is comprehensively portrayed (Fig. 2). The topologies are divided into three groups according to their logical relationships: 1) *Individuals*: individual e-spin nanomaterials with various inner or surface morphology; 2) *Hybrids*: incorporating functional nanomaterials or components into *Individuals*; and 3) *Assemblies*: hierarchical structures assembled from *Individuals* and/or *Hybrids*. Each group is further divided into several clusters. Specifically, their logical relationships are displayed by the direction of arrows in Fig. 2, in which *Individuals* form *Hybrids* by incorporating functional nanomaterials or active components; *Individuals* and *Hybrids*, as “Lego bricks”, are combined to form *Assemblies*.

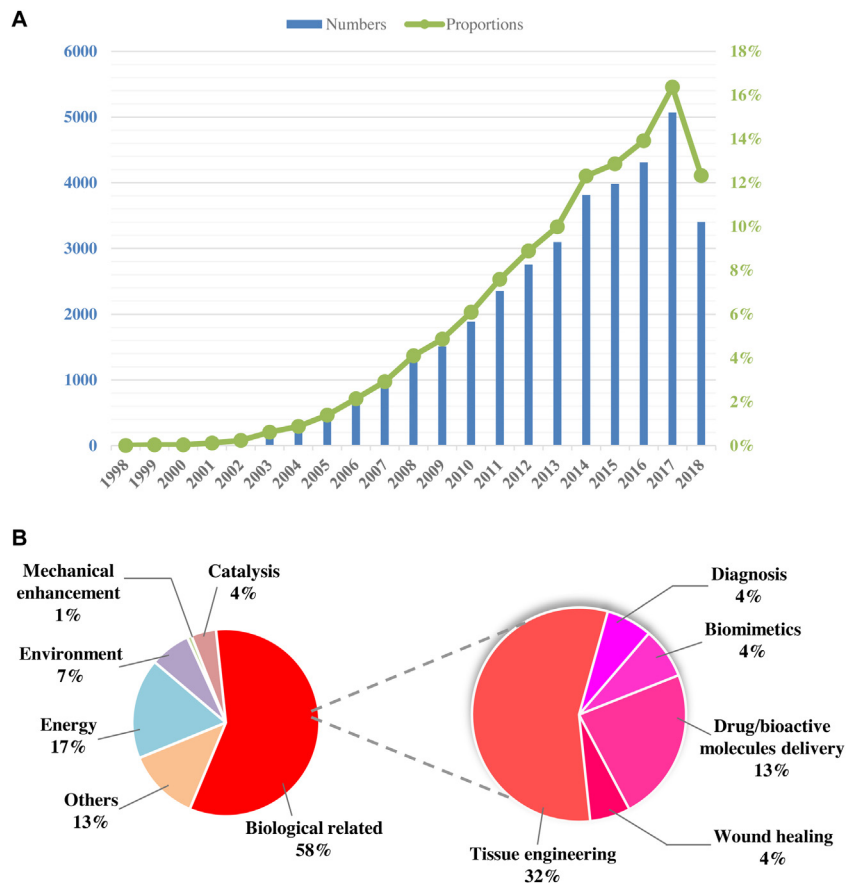


**Fig. 1.** (A) Number and proportion of scientific publications in last two decades, with the keywords “electrospinning” or “electrospun” (Source from ISI web of science, as of the end of August 2018). (B) Statistics of the literatures published in different application fields, and distribution of five major applications in biological field.

## 2.1. Individuals

Individuals are divided into three clusters. In cluster 1, bead, beaded fiber and fiber were the most three basic morphologies, primarily dependent on the concentration of polymer solutions [44]. In cluster 2, hollow, core-shell and multichannel structures possessed complex interior structures as compared to solid fibers. In general, these morphologies were fabricated by designing complex spinnerets [45–48]. In cluster 3, porous fibers and microcage possessed porosity and high specific surface area [49–51]. Porous and microcage nanomaterials were fabricated by phase separation, emulsion e-spin, changing substrates or regulating environmental humidity [52,53].

### 2.1.1. Bead, beaded fiber and fiber

With the increment of the concentration of polymer solution, the morphology evolved from beads, beaded fibers to fibers [54,55]. For example, beads, beaded fibers and fibers were prepared by adjusting the concentration of polycarbonate (PC) (Fig. 2-Bead, beaded fiber and fiber) [44]. When PC concentration was 8%, beads were fabricated. As PC concentration changed from 8% to 10% and 12%, beaded fibers and fibers formed, respectively. Moreover, cationic surfactants aided the formation of smooth and uniform PC nanofibers. Besides polymer concentration, surface tension and charge density of polymer solutions played critical roles in the formation of beaded fibers (Table 1) [54]. With the decrease of surface tension and charge density, the morphology of e-spin nanomaterials changed from beaded fibers to fibers. For instance, Greiner et al. demonstrated that fibers with beads arranged like flat ribbons on a string were formed by adjusting surface tension and viscosity

[20]. Besides, a large number of methods were utilized to regulate and control the shapes and dimensions of beaded fibers, such as changing geometry of the electrodes, field strength, feeding rate of polymer solution, vapor pressure of solvent, relative humidity and substrate type [56,57]. Concerning the selection of materials, a variety of natural or synthetic polymers were processed to beads, beaded fibers and fibers, such as chitosan, poly(ethylene oxide), poly(lactide-co-glycolide), chitosan/poly(vinyl alcohol), cellulase, poly(vinyl alcohol), and poly(vinyl alcohol) [56–59].

### 2.1.2. Hollow, core-shell and multichannel

Nanomaterials with complex interior structures had great potential for applications in a range of fields due to their distinctive anisotropy, large specific surface area, high adsorption and transport efficiency [60]. Coaxial e-spin was the most straightforward method to produce hollow, core-shell and multichannel nanomaterials. Regarding coaxial e-spin setup, two or more spinnerets applied with the same voltage were aligned-arranged in a concentric configuration [61,62]. Besides, coating or etching interior polymer of e-spin nanomaterials was another strategy to fabricate complex interior structures [45,63].

Coaxial e-spin was firstly reported in 2002 [47]. Using the setup with two spinnerets aligned-arranged in concentric configuration, micro- or nano- scale coaxial and immiscible fibers were generated. Coaxial e-spin was further developed to fabricate nanomaterials with complex interior structures. As the increment of structural complexity of spinnerets, hollow, core-shell and multichannel structures were obtained. Specifically, hollow structure was prepared using a special setup, in which one spinneret was concentrically inserted into another larger spinneret (Fig. 3A) [46].

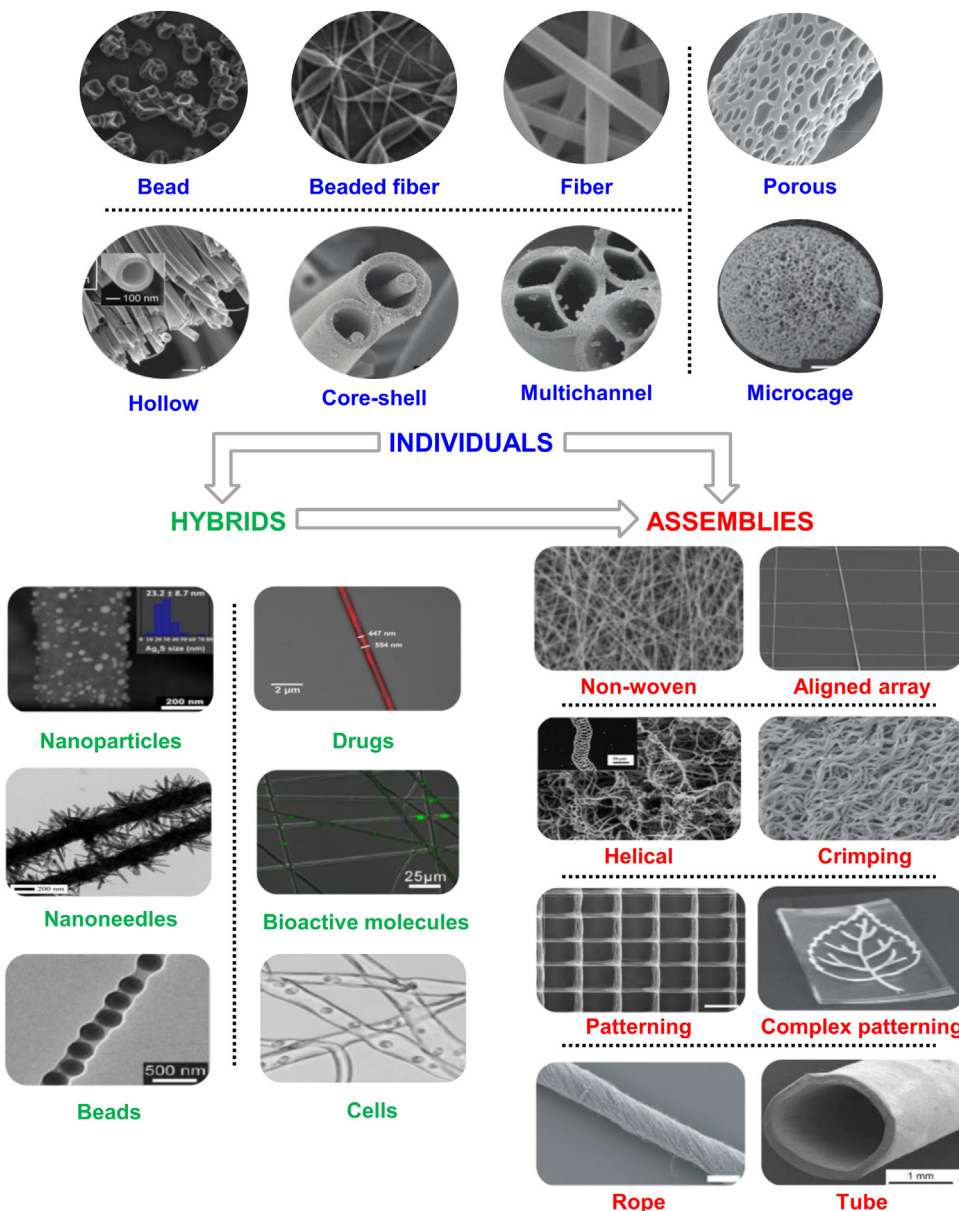


**Fig. 2.** “Topology periodic table” of e-spin nanomaterials. The topological structure of e-spin nanomaterials is categorized to *Individuals*, *Hybrids* and *Assemblies*. Images are modified from the original figures in the literature, Bead [44], Beaded fiber [44], Fiber [44], Hollow [46], Core-shell [64], Multichannel [65], Porous [79], Microcage [51], Nanoparticles [99], Nanoneedles [102], Beads [103], Drugs [121], Bioactive molecules [127], Cells [147], Non-woven [173], Aligned array [177], Helical [191], Crimping [197], Patterning [211], Complex patterning [212], Rope [219], Tube [225]. Sources: [44], Copyright 2009. Reproduced with permission from Springer-Verlag GmbH; [46,65,103,147], Copyright 2004, 2007, 2010, 2015, respectively. Reproduced with permission from the American Chemical Society; [64,177,197,212,219], Copyright 2010, 2007, 2015, 2017, respectively. Reproduced with permission from Wiley-VCH; [51,102,173], Copyright 2010, 2011, 2010, respectively. Reproduced with permission from the Royal Society of Chemistry; [79,99,211], Copyright 2017, 2017, 2015, respectively. Reproduced with permission from the Nature Publishing Group; [121,127,225], Copyright 2008, 2016, 2013, respectively. Reproduced with permission from Elsevier Ltd; [191], Copyright 2004. Reproduced with permission from American Institute of Physics.

**Table 1**

Influence of experimental parameters on the formation of beads, beaded fibers and fibers [54].

Solution viscosity (centipoise)	Morphology	Solution surface tension (mN/m)	Morphology	Charge density carried by the jet ( $\Omega \cdot \text{m}$ )	Morphology
13	Bead	75.8	Beaded fiber	83.4	Beaded fiber
74	Beaded fiber	68.9	Beaded fiber	47.4	Beaded fiber
160	Beaded fiber	63.1	Beaded fiber	16.7	Beaded fiber
289	Beaded fiber	59.3	Beaded fiber	3.61	Fiber
527	Fiber	54.7	Fiber	1.90	Fiber
1250	Fiber	50.5	Fiber	0.462	Fiber

For example, Li et al. loaded heavy mineral oil and titanium dioxide ( $\text{TiO}_2$ )/poly(vinyl pyrrolidone) (PVP) dissolved in ethanol solution into the inner and outer spinnerets, respectively. The mineral oil inside nanofibers was extracted in octane, forming the sheath fiber

with hollow structure (Fig. 2-Hollow). Alternatively, hollow fibers with polymeric sheath and empty inner phase (air) were achieved [61]. In addition, inorganic nanotubes were prepared by combining coaxial e-spin and post thermal treatments [66]. For instance,

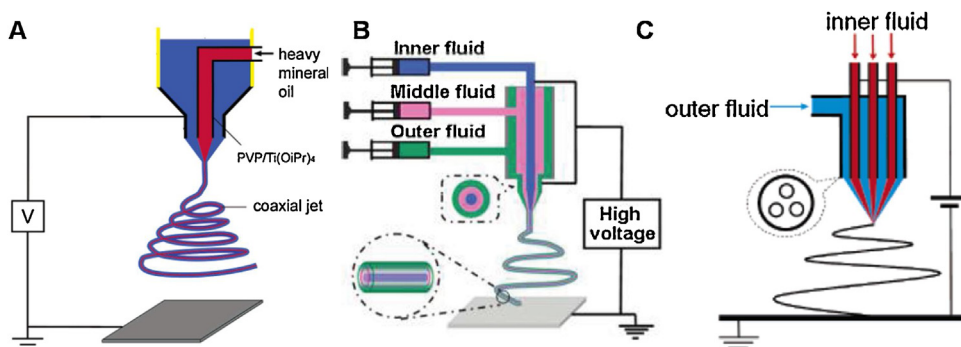


**Fig. 3.** Schematic illustration of the setup for fabricating e-spin nanomaterials with hollow, core-shell or multichannel structures. A: hollow [46]; B: core-shell [64]; C: multichannel [65]. Sources: [46], [65], Copyright 2004, 2007, respectively, reproduced with permission from the American Chemical Society; [64], Copyright 2010, reproduced with permission from Wiley-VCH Verlag.

Liu et al. fabricated hollow hierarchical zeolite fibers [67]. Specifically, a suspension of zeolite in PVP/ethanol solution served as outer fluid, while paraffin oil worked as inner fluid. As paraffin oil was immiscible in PVP solution, nanofibers with two-phase structure were obtained. Hollow structures were fabricated via calcination and removal of inner paraffin oil. Besides, multilayered and more complex hollow nanomaterials were prepared by using a tri-layered core-cut spinneret [68]. Core-shell nanomaterials were fabricated with the combination of post-treatments and three-coaxial spinneret. The three-coaxial spinneret was assembled from three concentric capillaries, through which three different fluids were fed to form a whole jet (Fig. 3B) [64]. TiO<sub>2</sub> dissolved in ethanol solution served as inner and outer fluid, and water/paraffin oil mixed emulsion worked as middle fluid which separated the inner and outer fluids. By applying high voltage, the conductive outer fluids were stretched, corporately driving inner and middle fluids to form nanofibers with sandwich structures. Subsequently, core-shell nanofibers were fabricated by calcination and removal of the organic components (Fig. 2-Core-shell). Further, inspired by the feathers of birds, Zhao et al. embedded multi-spinnerets in one needle and prepared nanofibers with multichannel structures (Fig. 2-Multichannel) [65]. Specifically, three equal spinnerets were embedded in a needle at three vertexes of the needle. The immiscible outer and inner fluids were separately injected into respective tubes and then the mixed jet was split into nanofibers. Multichannel structures were further fabricated by calcinating and removing the organic components (Fig. 3C). Similarly, nanofibers with both multichannel structures and multi-components were fabricated by using multi-fluidic compound-jet e-spin [69].

### 2.1.3. Porous and microcage

Porous nanomaterials were very useful in many fields due to their large specific surface area [70,71]. In general, porous e-spin nanomaterials were fabricated by phase separation and selective removal of one component through post treatments (Table 2) [72–76]. E-spin nanomaterials with smooth surfaces were directly prepared from homogeneous polymer solutions, whereas porous structures were usually obtained from heterogeneous polymer solutions with phase separation [77]. For example, porous poly(glycolic acid) (PGA)/poly(L-lactic acid) (PLA) nanofibers were fabricated from heterogeneous polymer solutions, in which PLA and PGA were immiscible [74]. Controlling the evaporation of solvent was a powerful way to form and regulate the porous structures. Using supercritical drying, solvent phase was selectively evaporated, forming polymer-based mesoporous structures [78]. Similarly, cryogenic liquid bath and subsequent drying induced the formation of porous structures [53]. Due to the phase separation of polymer and solvent, solvent islands within the solid fibers formed.

Immersing the fibers into cryogenic liquid froze the solvent islands rapidly without destruction, and subsequent drying in vacuum resulted in the formation of porous fibers. In addition, a simpler way to control the evaporation of solvent was adjusting ambient humidity [52]. In high-humidity environment, porous structures formed as a result of phase separation. High humidity promoted the formation of water islands which were immiscible with polymers, and subsequent drying resulted in forming porous structures. Besides, temperature was tuned to adjust solvent evaporation to induce phase separation, yielding porous structures (Fig. 2-Porous) [79]. On the whole, a variety of factors had effects on the formation of porous nanomaterials, including diffusion coefficients of solvents, solubility of polymers and the interaction between polymers and solvents [80].

Microcage was a special type of porous structures. Unlike other template or polymer emulsion methods to produce microcage with solid cores, microcage fabricated by e-spin was connected by fibers, thus forming macro-level three dimensional (3D) polymer networks (Fig. 2-Microcage) [51]. In detail, polymer-based blend emulsion solution with phase separation was prepared first; due to the difference of solvent evaporation rate, microcages formed in the process of e-spin. Alternatively, microcages were fabricated by combining emulsion e-spin and thermal treatments [81]. Polymer-based emulsion was first prepared by introducing TiO<sub>2</sub>/PVP/paraffin oil into tetrabutyl titanate solution; afterwards, the mixed emulsion was electrospun, and the obtained products were calcined at high temperature, removing organic components and forming microcages.

## 2.2. Hybrids

Incorporating desired functional moieties into *Individuals* renders e-spin nanomaterials with functions, generating *Hybrids*, which exhibit intriguing properties and unexpected potential for a variety of applications [82]. We categorize *Hybrids* into two clusters according to the property of the adding moieties: non-bioactive and bioactive components. Non-bioactive nanomaterials mainly included nanoparticles, nanoneedles and beads. Bioactive components contained drugs, bioactive molecules and cells. In particular, to cater for specific biological applications, assortments of bioactive components were encapsulated in the e-spin mats, including antibiotics, cytostatics, therapeutic drugs, proteins, growth factors, polypeptide, microRNA, DNA, small interfering RNA, cells, bacteria and fungus [83].

### 2.2.1. Nanoparticles, nanoneedles and beads

There are two major methods to fabricate e-spin nanomaterials encapsulated with nanoparticles, nanoneedles or beads (Table 3). The first method includes two steps: e-spin of poly-

**Table 2**

Strategies for the preparation of porous e-spin nanomaterials.

Polymer materials	The occurrence of phase separation	Post treatments (selective removal of one component)	Literature
Polystyrene	Yes	No	[52]
Polystyrene	Yes	Liquid nitrogen bath and drying	[53]
Polylactide/polyvinylpyrrolidone	Yes	Solvent extraction	[72]
Gelatin/polycaprolactone	Yes	Extracted by phosphate buffered saline	[73]
Poly(glycolic acid)/poly(L-lactic acid)	Yes	Extracted by chloroform	[74]
Polyacrylonitrile/polyvinylpyrrolidone	Yes	Supercritical drying	[78]
Polycaprolactone	Yes	No	[79]

**Table 3**

Strategies for the preparation of e-spin nanomaterials encapsulated with nanoparticles, nanoneedles or beads.

Non-bioactive nanomaterials	Post processing strategy	Literature
$\text{V}_2\text{O}_5$ nanoneedles	Grown on rutile precursor nanofibers by calcinations	[88]
$\text{ZnO-SnO}_2$ nanoparticles	Calcinating $\text{Zn}(\text{NO}_3)_2/\text{SnCl}_2$ precursor polymer fibers	[87]
Sb nanoparticles	Calcinating $\text{SbCl}_3/\text{polyacrylonitrile}$ as-spun fibers	[86]
Metal nanoparticles	Calcinating metal salt doped polymer based fibers	[85]
Tin-doped indium oxide nanoparticles	Calcinating $\text{SnCl}_4/\text{In}(\text{NO}_3)_3/\text{polyacrylonitrile}$ as-spun fibers	[92]
$\text{NiSe}_2$ nanoparticle	Selenization of composite fibers at 300 °C under $\text{H}_2\text{Se}$ gas	[94]
$\text{PbS}$ nanoparticles	Gas-solid reaction of polymer/lead ion fibers under $\text{H}_2\text{S}$ gas	[95]
$\text{TiO}_2$ nanoneedles	Grown on titanium isopropoxide nanofibers by calcinations	[102]
$\text{SiO}_2$ beads	Introducing $\text{SiO}_2$ beads in polymer solution for e-spin	[103]
$\text{ZnO}$ beads	Introducing $\text{ZnO}$ beads in solution for near-field e-spin	[104]

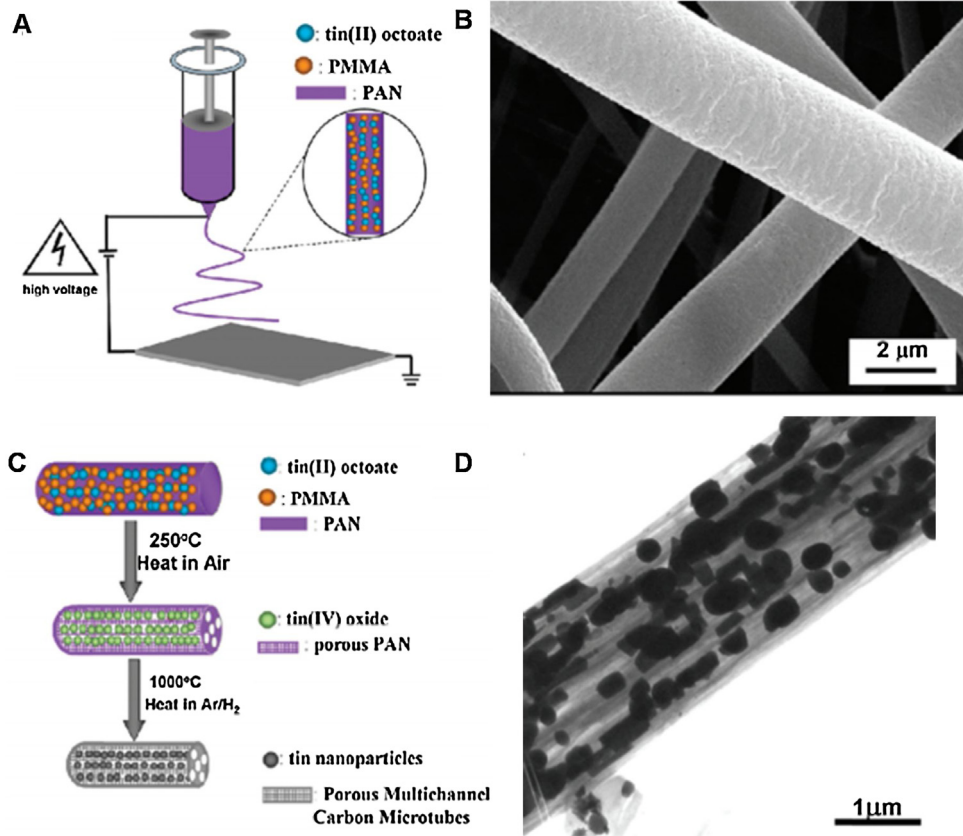


**Fig. 4.** (A) Schematic illustration for the fabrication process of poly(methyl methacrylate) (PMMA)/ polyacrylonitrile (PAN)/Sn ions nanofibers. (B) SEM images of the corresponding nanofibers. (C) Schematic illustration of preparing Sn nanoparticles-doped carbon-based nanofibers. (D) SEM images of the corresponding nanofibers. [84], Copyright 2009. Reproduced with permission from the American Chemical Society.

mer solution containing the precursors, and post treatments such as calcinations [84–92], laser ablation [93], selenization [94], and gas-solid reaction [95–98]. For example, smooth polymer/Sn ions nanofibers formed first (Fig. 4A and B), and the following calcination process converted Sn ions inside nanofibers to Sn nanoparticles (Fig. 4C and D) [84]. Similarly, other metal nanoparticles-doped nanofibers were prepared using this method. Specifically, solutions

of metal salts/polyvinyl alcohol (PVA) were electrospun first, yielding nanofibers; and the nanofibers were subsequently calcined at 400 °C in argon (Ar) atmosphere, forming nanofibers doped with metal nanoparticles [85]. Besides calcinations, gas-solid reaction was another post treatment way to prepare nanoparticles doped e-spin nanomaterials [95]. In detail, lead acetate and cadmium acetate dissolved in PVP solution were electrospun first, and then

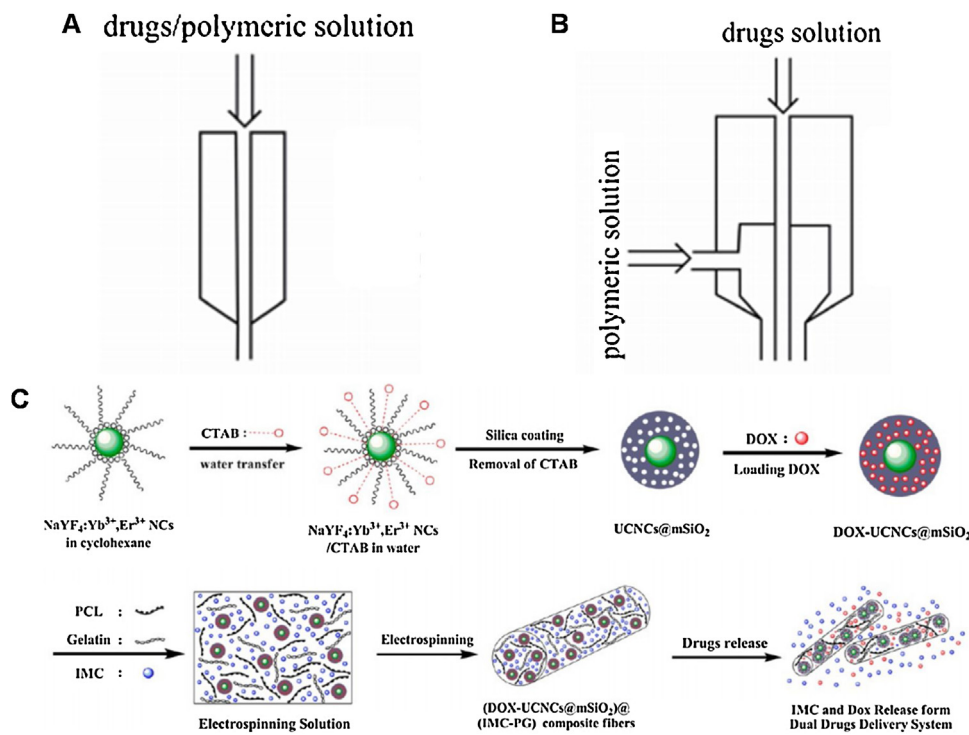


**Fig. 5.** Schematic illustration of the three kinds of methods for fabricating drugs encapsulated nanofibers. A: e-spin using single nozzle; B: coaxial e-spin using dual nozzle [119]; (C) Fabrication of drugs encapsulated nanoparticles, and then the polymer matrix containing nanoparticles were electrospun [120]. Sources: [119], Copyright 2015. Reproduced with permission from Springer Nature; [120], Copyright 2013. Reproduced with permission from the American Chemical Society.

the resultant nanofibers were exposed to sulfuretted hydrogen ( $\text{H}_2\text{S}$ ) gas to form lead sulfide ( $\text{PbS}$ ) nanoparticles. Further, two-step post treatments were employed to prepare silver sulfide ( $\text{Ag}_2\text{S}$ ) nanoparticles doped  $\text{TiO}_2$  nanofibers, including reduction of  $\text{Ag}^+$  to  $\text{Ag}$  followed by sulfurization of  $\text{Ag}$  to  $\text{Ag}_2\text{S}$  (Fig. 2-Nanoparticles) [99].

Another more straightforward method was to mix polymer and as-received nanoparticles directly. For instance, zirconia ( $\text{ZrO}_2$ ) doped polymer nanofibers were prepared by directly e-spin polymer solution with  $\text{ZrO}_2$  nanoparticles [100]. Moreover, these two methods were combined to fabricate hybrid nanofibers with multi-components. For example, Kim et al. fabricated  $\text{TiO}_2$  nanofibers containing two kinds of nanoparticles, where Pt nanoparticles were directly doped and Nb nanoparticles were formed by post-calculinations [101].

Nanoneedles doped e-spin nanomaterials were usually fabricated by *in situ* growth strategy, such as hydrothermal assisted *in situ* growth process or *in situ* reduction process [88]. For example, Meng et al. fabricated  $\text{TiO}_2$  nanoneedles doped anatase nanofibers by immersing nanofibers in titanium isopropoxide/hydrochloric acid (HCl), followed with a subsequent hydrothermal reaction (Fig. 2-Nanoneedles) [102]. E-spin beads in polymer solutions generated necklace-like nanomaterials. In general, beads doped e-spin nanomaterials were fabricated by directly e-spin polymer solutions with beads. For example, Jin et al. prepared silicon dioxide ( $\text{SiO}_2$ ) beads doped PVA fibers through directly introducing  $\text{SiO}_2$  beads in PVA solution (Fig. 2-Beads) [103]. Various factors including the diameter of  $\text{SiO}_2$  beads, weight ratio of PVA to  $\text{SiO}_2$  beads, and the e-spin voltage had the effects on the formation of necklace-like structures. Similarly, other beads doped nanomaterials were fabricated using the modified e-spin methods, such as near-field e-spin [104] and gradient e-spin [105].

Compatibility such as wettability and size between polymers and inorganic particles played vital roles in preparing non-bioactive e-spin nanomaterials. In general, the wettability of inorganic par-

ticles should be consistent with the solvents and matrix polymers. Jin et al. demonstrated that  $\text{SiO}_2$  beads were compatible with PVA and water, however, polystyrene beads were hydrophobic so that aggregation formed [103]. Similarly, Zhang et al. demonstrated that inorganic particles should be pre-treated to form a compatible layer on the surface prior to being added into polymer solutions, so as to improve the wettability and prevent aggregation [106]. Specifically, a small portion of polymers were first added to inorganic particle dispersions to form polymer coatings, thus preventing aggregation, and then the rest of polymers were added. Another important factor was the size of inorganic particles. When the diameter was far smaller than that of fibers, nanoparticles were uniformly dispersed; while when the diameter was increased to a critical value (140 nm), the nanoparticles tended to aggregate to minimize the surface tension [103,107]. Post-treatments, such as hydrothermal reactions [102,108–110], surface treatments [111–113], or *in situ* reduction [114–117] were effective to improve the dispersity of nanoparticles in polymers. In addition, nanoparticles and beads were directly absorbed on the surface of e-spin mats via hydrogen bonding, electrostatic force or the interactions among functional groups [118]. For example, hollow graphitic carbon nanospheres were directly absorbed on the surface of e-spin nanofibers by immersing the fibers in carbon nanoparticle solutions [111].

## 2.2.2. Drugs, bioactive molecules and cells

Compared with other drug delivery systems, drugs loaded in nanofibers had unique features, such as high surface-to-volume ratios and simple fabrication process [119]. In general, there were two main methods to fabricate drugs loaded e-spin nanomaterials. Drugs were directly mixed with polymer solution first, and then the polymer solution containing drugs was directly electrospun (Fig. 5A) [119]. Alternatively, drugs solution and polymer solution were served as inner and outer layer of the spinneret for coaxial e-spin, respectively (Fig. 5B). Similarly, emulsion e-spin was an effective method to fabricate drugs loaded nanomaterials.

**Table 4**

E-spin nanomaterials of polymer/bioactive molecules.

Bioactive molecules	Functions	Literature
Keratin peptides	Protection for animal/plant cells	[132]
siRNA	Suppression of target gene expression	[133,134]
Plasmid DNA	Regulating cell proliferation and differentiation	[135,136]
Growth factor	Regulating cell proliferation and differentiation	[137]
Therapeutic proteins	Repairing of tissue injury	[138]
miRNA	Interference of gene expression	[139]
Viruses	Regulating cell metabolism	[140]

For example, direct e-spin of poly(ethylene glycol)-poly(L-lactic acid)/drugs mixed emulsion solution generated nanofibers with drugs distributed in the center of nanofibers (Fig. 2–Drugs) [121]. In order to achieve more controllable release fashion, drugs were loaded in nanoparticles and the diffusion of drugs were tuned by adjusting the distribution of drugs in nanoparticles. For instance, doxorubicin (DOX) was loaded in core/shell silica nanoparticles, and then the DOX doped nanoparticles and indomethacin (IMC) were encapsulated inside poly( $\epsilon$ -caprolactone)-gelatin nanofibers [120]. In this system, IMC released faster than DOX due to their different distributions in e-spin nanomaterials. Regarding the driving force of drugs loading, physical adsorption and chemical linking were the two main interactions to prepare drugs loaded e-spin nanomaterials [122]. For example, antibiotics were physically adsorbed on polyhydroxybutyrate (PHB) nanofibers, and the resultant hybrid nanofibers possessed antimicrobial capability [123].

A large number of bioactive molecules were incorporated in e-spin nanomaterials (Table 4). In general, the preparation strategy was similar to that of fabricating drugs loaded e-spin nanomaterials, including direct e-spin, coaxial e-spin [124], emulsion and suspension e-spin [125]. For example, peptide-modified poly(ethylene glycol)-b-poly(L-lactide-co- $\epsilon$ -caprolactone) (PELCL) nanomaterials were fabricated through direct e-spin [126]. Specifically, PELCL e-spin mats were fabricated using direct e-spin, followed by immersing the e-spin mats in the polypeptide solutions. Moreover, bilayer e-spin mats loaded with microRNA were prepared using emulsion and dual-power e-spin (Fig. 2–Bioactive molecules) [127]. PELCL/microRNA emulsion solution was prepared and electrospun to fabricate microRNA loaded PELCL e-spin mats. Then poly ( $\epsilon$ -caprolactone) (PCL) and gelation mixed solutions were electrospun on the surface of PELCL mats as outer layer. Similarly, in order to achieve more controlled release manner, nano-containers were utilized to package bioactive molecules [128–130]. For example, platelet-derived growth factor (PDGF) and vascular endothelial growth factor (VEGF) were encapsulated into collagen nanoparticles, and then the bioactive nanoparticles were dispersed in hyaluronic acid solution for e-spin [131].

Incorporating organisms such as cells into e-spin nanomaterials generated new types of functional materials, so-called living materials [141–148]. In 2006, Charles et al. first demonstrated that bacteria and virus were encapsulated in e-spin fibers [146]. The bacteria encapsulated in e-spin fibers remained viable for more than three months at  $-20^{\circ}\text{C}$ . Moreover, *Micrococcus luteus* (*M. luteus*) with high genome GC content survived for more than 15 days in e-spin fibers at room temperature using poly(ethylene oxide) (PEO) as polymer matrix [141]. As the diameter of cells was a few microns, direct e-spin was difficult to encapsulate cells very well. Coaxial e-spin was therefore utilized to encapsulate living cells inside fibers using polymer matrix as the outer layer [149]. Besides, hydrogel micro-particles were utilized to encapsulate bacterial cells, and then micro-particles/polymer solution were electrospun to prepare cells loaded electrospun mats [148]. Porous structures were also used to encapsulate cells [145]. Letnik et al. fabricated

bioactive fibers with yeast cells embedded in the shell of polymer matrix (Fig. 2–Cells) [147]. The obtained living fibers were used for ethanol production, demonstrating the activity of cells. Similarly, core–sheath fibers encapsulated with red blood cells were prepared using coaxial e-spin, and the cells maintained cellular integrity and functions inside fibers [150].

### 2.3. Assemblies

Hierarchical structures were fabricated from *Individuals* and/or *Hybrids*, resulting in *Assemblies*. And *Assemblies* with re-entrant texture at both the coarser and the finer length scales met all kinds of requirements of biological applications [151,152]. As the complexity of topological structures increased, *Assemblies* were categorized to four clusters. In cluster 1, non-woven structure was the most common topology with unprecedented porosity, which was used to mimic the structure of natural extracellular matrices (ECMs) [153]. Aligned array structure with highly ordered architectures was usually fabricated by manipulating/changing the e-spin set-up or driving force [154,155]. In cluster 2, helical and crimping structures absorbed more components/strain than the straight counterparts, due to their flexible structures bending characteristics [156]. Various processing or post-treatment strategies were utilized to prepare helical or crimping fibers, such as charge neutralization induced viscoelastic contraction and solvent post-treatments. Notably, the surface tension was the key parameter that affected the formation of helical or crimping structures. In cluster 3, patterning and complex patterning structures with controllable shape and orientation were used to mimic some fibrous tissues such as connective tissues [157,158]. In general, changing configuration or surface architectures of the collectors was the easiest way to fabricate patterning or complex patterning e-spin nanomaterials [159,160]. In cluster 4, ropes and tubes were the most complex structures in *Assemblies*. Some methods were developed to prepare e-spin nanomaterials with rope or tube structures, such as multilayer e-spin, assembly by 2D electrospun fibrous mats or using suitable collectors as temples [161–163]. The most straightforward way was designing appropriate 3D collectors [164–169].

#### 2.3.1. Nonwoven and aligned array

In general, due to the bending instability of the jet formed during e-spin [170], nanofibers were routinely collected in the form of random orientation [169]. The formation of non-woven mats still needed to be controlled by optimizing the operational parameters [171], choosing different polymer systems and post-treatment methods [172]. For instance, mechanically stable non-woven mats were fabricated using epoxy as adhesive to generate junctions among nanofibers (Fig. 2–Non-woven) [173]. In detail, epoxy/curing agent/polymer mixed solutions were processed to form nanofibers, which were afterwards heated to allow epoxy resin curing. As a result, junctions formed among nanofibers, producing stable non-woven mats. In another way, plasma treatment was an easy, innovative and environmentally friendly post-treatment method to crosslink gelatin nanofibers, resulting in structurally stable non-woven mats [174]. In addition, polymer based non-woven mats were used as template to fabricate inorganic non-woven mats [175]. Specifically, silica precursor solution was mixed with PVA, and then PVA based non-woven mats were prepared using e-spin. In this case, PVA was served as the template to immobilize the distribution of silicon element. Subsequently, the obtained non-woven mats were calcined at high temperature to remove PVA, forming fully inorganic silica non-woven mats.

Aligned array nanomaterials were prepared through a variety of methods, which were mainly emphasized on the modifications of the setups, especially the specific counter electrode configuration [179,180]. In general, these methods were categorized into three

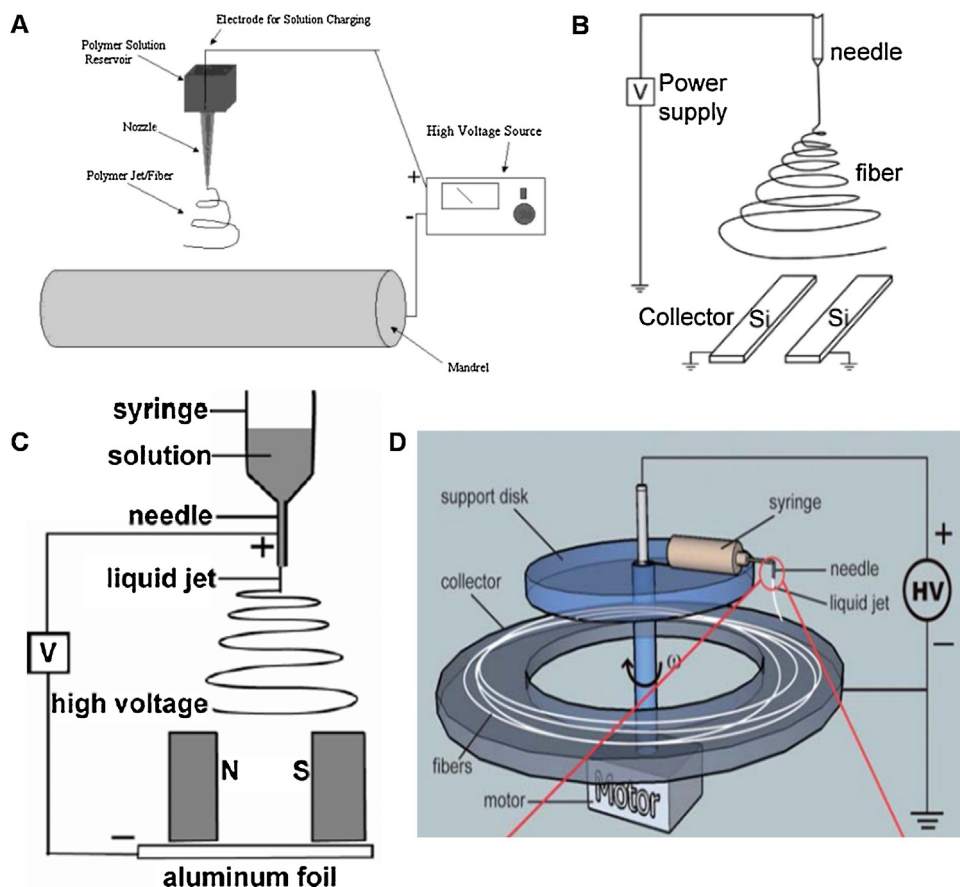


**Fig. 6.** Schematic illustration for the preparation strategies of aligned array nanomaterials. (A) Fiber arrangement was controlled by adjusting the motion of the grounded mandrel [176]; (B) Two pieces of conductive silicon stripes separated by a gap were served as collectors [159]; (C) Two pieces of permanent magnets positioned on the aluminum foil were served as the collectors [177]; (D) The spinneret fixed on a support disk was attached to a motor to generate centrifugal force during e-spin [178]. Sources: [159,176], Copyright 2002, 2003, respectively. Reproduced with permission from the American Chemical Society; [177], Copyright 2007. Reproduced with permission from Wiley-VCH; [178], Copyright 2011. Reproduced with permission from the Royal Society of Chemistry.

**Table 5**

Strategies for the fabrication of aligned array e-spin nanomaterials.

Materials	Fabrication strategy	Literature
Poly(vinyl pyrrolidone)	Introducing two pieces of conductive silicon strips separated by a gap	[159]
Poly(vinyl alcohol)	Introducing a cylinder collector rotated at a high speed	[168]
Nylon-6	Introducing a circular drum composed of evenly spaced copper wires	[179]
Collagen	Introducing the grounded mandrel rotated at high speed	[176]
Polystyrene	Introducing an insulating cylinder attached to a motor	[182]
Poly(ethylene oxide)	Introducing a tapered and wheel-like bobbin	[184]
Poly(vinyl alcohol)	Introducing two pieces of magnets on the collectors	[177]
Polystyrene	The spinneret was fixed on a support disk attached to a motor	[178]
Polyacrylonitrile	Rotating e-spin apparatus composed of hollow cylinder	[186]
Polyacrylonitrile	Rotating e-spin apparatus composed of two concentric hollow cylinders	[187]

types: (a) adopting the rotating collectors, such as rotating drums, cones and cylinders [168,176,181–184]; (b) precisely manipulating auxiliary electric field or magnetic field [159,177,178,185]; (c) using centrifugal e-spin which combined electrical and centrifugal forces during e-spin [186,187]. Matthews et al. first observed and regulated the alignment of collagen fibers using rotating mandrel [176]. The e-spin setup included high voltage source, grounded mandrel, and the spinneret. Fiber arrangement and orientation were controlled via adjusting the motion of the grounded mandrel (Fig. 6A). However, the degree of alignment declined as time went on and too many fibers accumulated on the mandrel. It was interpreted that the accumulation of residual charges on the previously collected nanofibers interfered with the alignment of the new nanofibers. To improve the degree of alignment, two pieces of electrically conductive silicon stripes separated by a

gap were introduced as collectors to prepare aligned nanofibers for a longer period (Fig. 6B) [159]. During e-spin, the charged nanofibers were stretched to spin across the gap, forming aligned array nanofibers over large areas. In a different way, Yang et al. developed a magnetic e-spin method to fabricate well-aligned and large area ( $5\text{ cm} \times 5\text{ cm}$ ) e-spin mats using the auxiliary magnetic field, wherein the charged jet was magnetized by the addition of ferroferric oxide ( $\text{Fe}_3\text{O}_4$ ) magnetic nanoparticles (Fig. 2-Aligned array) [177]. Two pieces of permanent magnets positioned on the aluminum foil were served as collectors and the arrangement of nanofibers was adjusted through regulating the arrangement of magnets (Fig. 6C). In addition, centrifugal e-spin was a powerful method to prepare aligned array nanomaterials. The spinneret fixed on the circular platform named “support disk” was attached to the

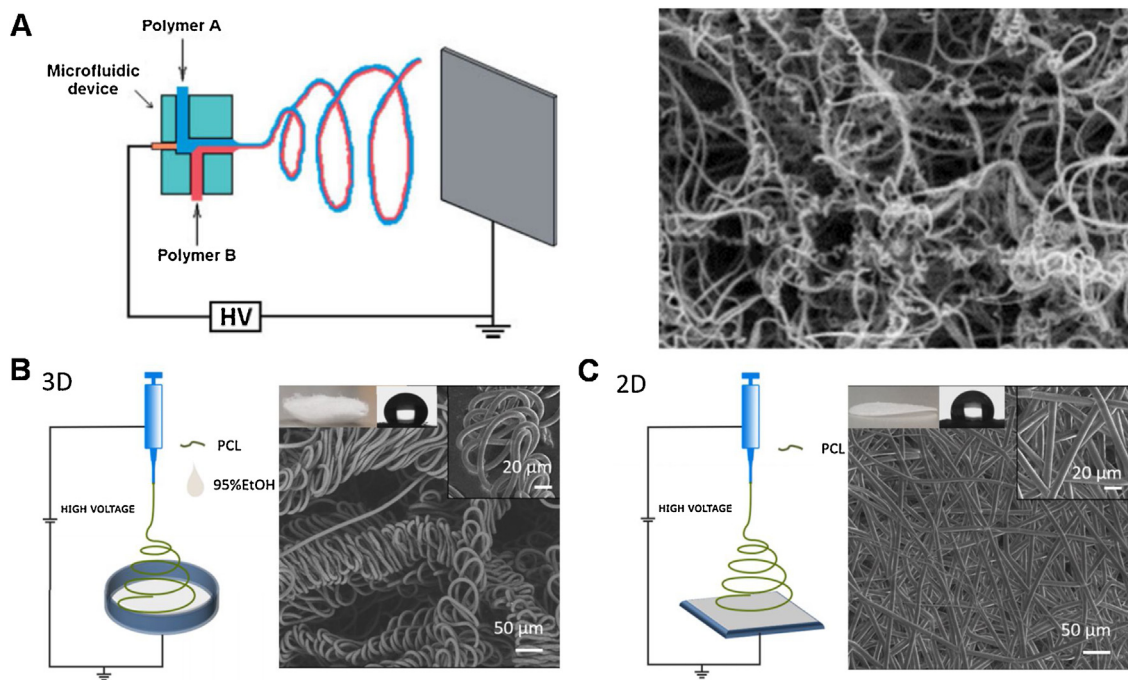


**Fig. 7.** Schematic illustration for the preparation strategies of helical e-spin nanomaterials. (A) The microfluidic device was served as the spinneret to fabricate side-by-side bicomponent helical nanofibers [151]; (B) Polycaprolactone (PCL) solution was directly electrospun to prepare 2D non-woven mats. (C) 3D helical PCL mats were fabricated using 95% ethanol solution to collect the resultant fibers [188]. Sources: [151], Copyright 2005. Reproduced with permission from Wiley-VCH; [188], Copyright 2016. Reproduced with permission from the American Chemical Society.

speed-adjustable motor, providing centrifugal force to regulate the arrangements of nanofibers (Fig. 6D) [178] (Table 5).

### 2.3.2. Helical and crimping

Surface tension was the key parameter that affected the formation of helical or crimping structures. Therefore, various processing or post-treatment strategies related to the change of surface tension were utilized to prepare helical or crimping nanomaterials [189,190]. In general, two kinds of polymers with different properties including elasticity or conductivity were electrospun to fabricate helical fibers. For example, helical fibers were fabricated via utilizing the difference of polymer conductivity (Fig. 2-Helical) [191]. First, conductive poly(aniline sulfonic acid) and nonconductive poly(ethylene oxide) were dissolved in water/methanol mixed solvents. Then the mixed solutions were electrospun to prepare helical fibers, due to the partial charge neutralization of charged fibers, followed by the viscoelastic contraction of the fibers. Similarly, two kinds of polymers including flexible thermoplastic polymer (polyurethane) and rigid thermoplastic polymer (Nomex®) were utilized to fabricate helical fibers, due to the differences of the polymer elasticity [192]. Moreover, the microfluidic device served as the spinneret was used to prepare side-by-side bicomponent helical e-spin nanofibers [151]. Elastomeric polymer (polyurethane) solution and thermoplastic polymer (polyacrylonitrile) solution were injected into microfluidic device from different entrances, and then the side-by-side bicomponent polymer mixed solution was formed. Due to the differences of polymer elasticity, helical nanofibers were formed during e-spin (Fig. 7A). In addition, solvent post-treatment was a simple method to fabricate helical fibers [188]. For instance, 3D helical PCL mats were prepared using 95% ethanol solution to collect the resultant fibers (Fig. 7B). As a control, 2D PCL non-woven mats were obtained by direct e-spin (Fig. 7C). Considering the formation mechanism, ethanol with low surface tension endowed fibers with good bending ability [193].

Crimping structures were highly anisotropic and similar to the structures of tendon, being used to transmit energy effectively

[194–196]. The preparation strategies were similar to those of helical fibers and the surface tension was the key parameter. For instance, the introduction of ethanol into PLA solution promoted to generate crimping fibers during e-spin (Fig. 2-Crimping) [197]. The degree of crimping was adjusted via changing the content of ethanol. The presence of ethanol helped release the residual stress of polymer chains and reduce system energy, leading to the generation of crimping fibers. In addition, the differential shrinkage/expansion induced by the external conditions, including temperature and humidity were employed to prepare crimping fibers [198].

### 2.3.3. Patterning/complex patterning

Patterning or complex patterning structures were prepared through various methods such as changing the configurations [199] or surface architectures [203–205] of the collectors, post-processing treatments of the as-spun membranes [200,206], near-field e-spin [201], conductive or nonconductive template assisted e-spin [207,208] and melt e-spin [202,209]. And the major way was designing the collectors with desirable patterns and protrusion arrangements [204,207,210]. For instance, patterned e-spin nanomaterials were fabricated using the collectors with specific configurations [199]. When the collector with equally spaced rectangular protrusions was utilized, the corresponding patterned architectures composed of nanofibers were obtained (Fig. 8A). And the stacking density of nanofibers was adjusted by changing voltages, feeding rates and volume ratio of solvents. Other types of patterned architectures including toothed, hexagonal and re-entrant structures were prepared using this method [204]. Post treatments of the as-spun membranes, such as the dissolving method was another way to fabricate personal patterned architectures [206]. Non-woven e-spin mats were prepared first, followed with partial dissolution of e-spin mats, forming patterned architectures. Similarly, Hu et al. proposed a reliable approach to pattern e-spin nanofibers via solvent-containing hydrogel stamps [200]. The process included four steps: 1) non-woven e-spin mats were

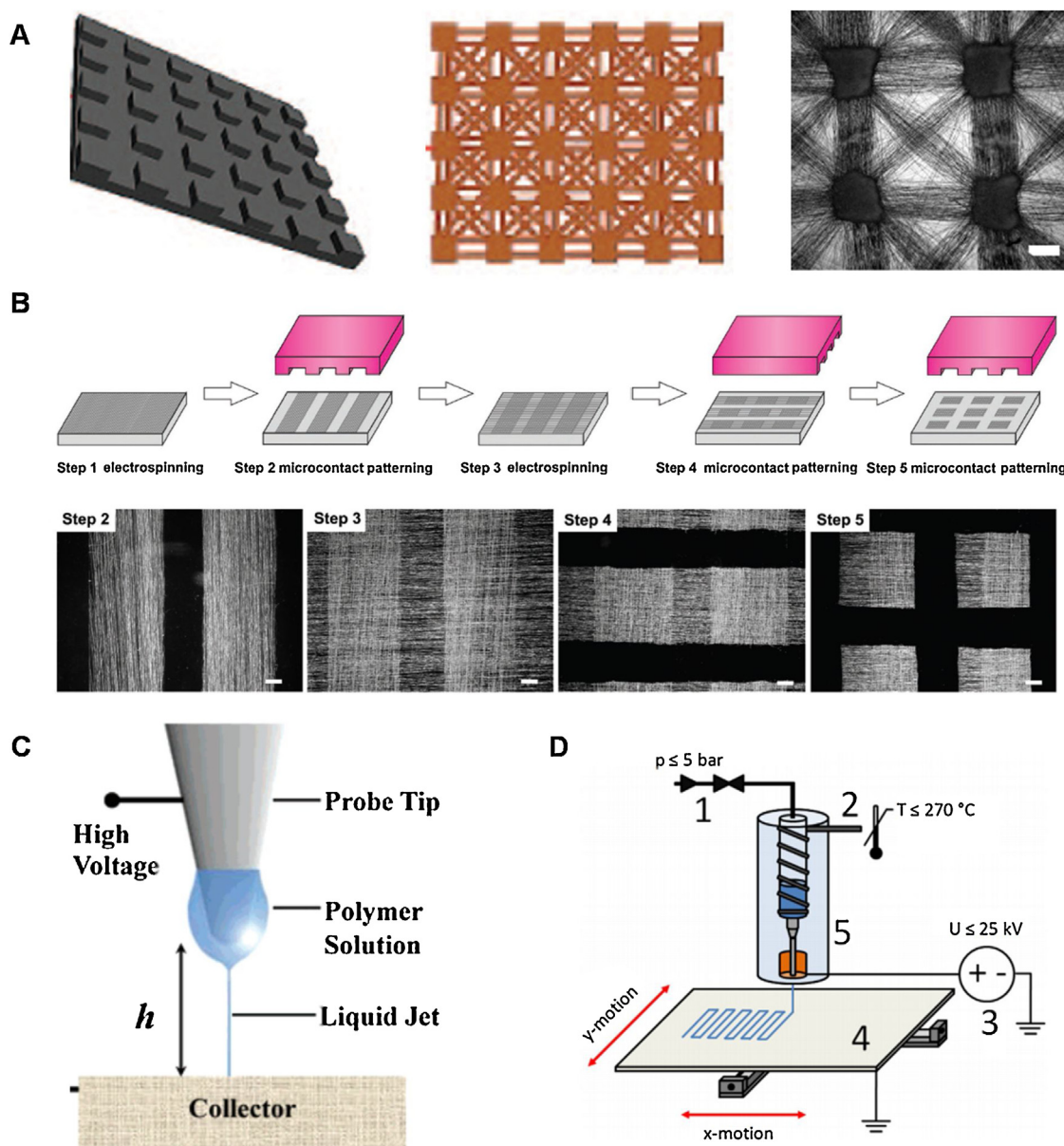


**Fig. 8.** Schematic illustration for the fabrication strategies of patterned nanomaterials. (A) (Left) Scheme for the collectors with equally spaced rectangular protrusions; (middle) scheme for the obtained fibrous patterned architectures; (right) SEM images of the patterned nanomaterials [199]; (B) Scheme for the fabrication process of patterned microstructures and the corresponding SEM images after each step [200]; (C) Scheme for the process of near-field e-spin. The polymer solution was attached to the tip of tungsten electrode to prepare electrospun patterned materials in a personal way [201]; (D) Scheme for the device of the melt e-spin. 1: feeding system; 2: heating system; 3: voltage source; 4: computer assisted collector; 5: spinneret, [202]. Sources: [199,201], Copyright 2008,2006, respectively. Reproduced with permission from the American Chemical Society; [200], Copyright 2017. Reproduced with permission from Wiley-VCH; [202], Copyright 2014. Reproduced with permission from Elsevier Ltd.

fabricated; 2) hydrogel stamps were utilized to partially dissolve the non-woven mats; 3) e-spin was continued to prepare the multiple mats; 4) hydrogel stamps were used to partially dissolve the mats in the vertical directions (Fig. 8B). Near-field e-spin was a direct and controllable way to fabricate patterned materials and the electrode-to-collector distance was narrowed down to 500  $\mu\text{m}$  [201]. The polymer solution was attached to the surface of tungsten electrode and the charged fibers were directly formed and written through applying high voltage (Fig. 8C). As the electric field force was the driving force during e-spin, conductive or nonconductive templates were utilized to prepare patterned e-spin nanomaterials [207]. For instance, conductive template with designable arrangements promoted the deposition of the charged fibers, forming patterned e-spin nanomaterials [208]. And the shape and diameter of conductive template played key roles in controlling the depo-

sition of fibers. Besides, melt e-spin involved computer-assisted deposition process, which produced patterned e-spin nanomaterials with rational designs [209]. Polymers were melted in heating system first, and afterwards the polymer liquid was split into fibers under high voltage (Fig. 8D) [202]. For example, patterned fibrous mats were fabricated through direct e-spin of the molten polymer liquids (Fig. 2-Patterning) [211].

Instead of the conventional simple patterned collectors, sophisticated collectors composed of electrolyte solutions and microcavities with curved surface were designed to prepare complex-patterning e-spin nanomaterials (Fig. 2-Complex patterning) [212]. Through the design of the shape and position of microcavities, e-spin nanomaterials with complex patterned structures were obtained. And the curved surface of the microcavities enabled the formation of 3D patterned structures. Regarding the

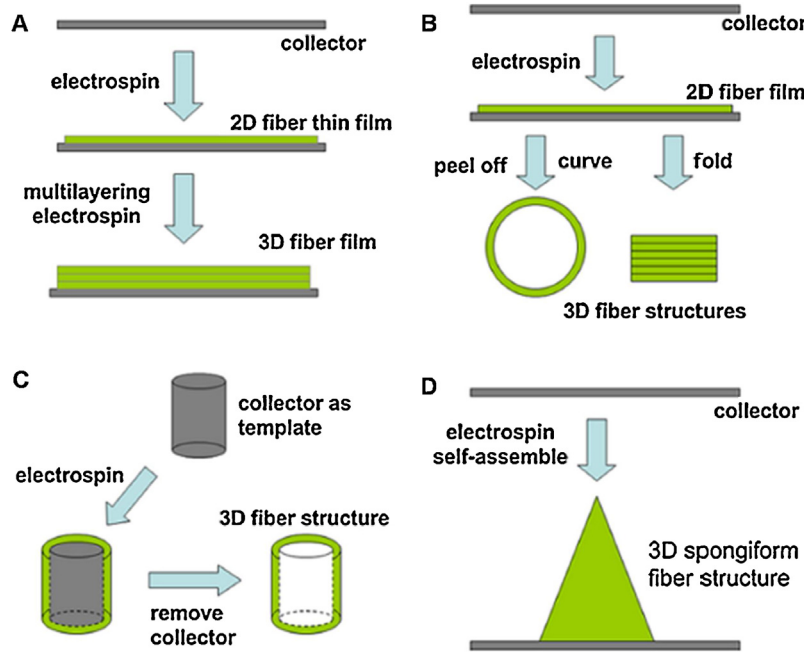


**Fig. 9.** Schematic illustration for the fabrication strategies of rope and tube structures. (A) Multilayer e-spin. (B) Assembly by post-processing of 2D e-spin fibrous mats. (C) Utilizing a 3D template to collect fibers. (D) Direct self-assemble by an auxiliary factor [214]. Copyright 2014. Reproduced with permission from Elsevier Ltd.

formation mechanism, the as-spun fibers were only deposited and floated on the air-liquid interface due to surface tension and electrostatic force. In addition, complex-patterning structures were adjusted and regulated via changing the e-spin time, voltage and the distance between the spinneret and collector [213].

#### 2.3.4. Rope and tube

Rope and tube structures were mainly fabricated via four e-spin strategies [214]: 1) multilayer e-spin; 2) assembly by post-processing of 2D e-spin fibrous mats; 3) utilizing a 3D template to collect fibers; 4) direct self-assembly by an auxiliary factor. In detail, multilayer e-spin was a simple but time-consuming method to prepare 3D fibrous structures. Millimeter-scale 3D e-spin mats were fabricated via stacking the fibers (Fig. 9A). Another way was to change 2D fibrous mats to 3D scaffolds by rolling up the fibrous layers. 2D e-spin mats were prepared, and then the mats were folded into 3D tubular scaffolds (Fig. 9B). Further, 3D collector with various shapes and sizes were used to fabricate 3D fibrous scaffolds. First, a 3D template was utilized to collect fibers. Then the 3D fibrous mats were formed through sacrificing the 3D template (Fig. 9C). Besides, other auxiliary factors such as liquid collectors were used to regulate the 3D self-assembly of the fibers (Fig. 9D). It was noteworthy that polymer concentration, applied voltage and ambient humidity were the key parameters to promote a rapid growth of the 3D fibrous mats [215]. The most straightforward way was designing appropriate 3D collectors [199]. For example, two grounding rings were utilized to collect the fibers suspended on the rings. Then the fibers were converted into multi-filament yarns through rotating the rings, yielding the rope structures [216]. Similarly, two mutually perpendicular spinnerets were utilized to fabricate the intertwined fibers, followed with the method of rope assembly, increasing the fiber packing density [217]. Furthermore, a Teflon drum was used to collect the graphene fibers which intertwined with each other to form rope-shape e-spin mats [218]. Notably, a rapid and point-of-use fiber manufacturing platform was developed to fabricate rope-shaped fibers (Fig. 2-Rope) [219]. The manufacturing platform was composed of a polymer reservoir and rotating collector

attached to the motor (Fig. 10A). When the collector was rotated at high speed, the collector was in close to the reservoir to induce the polymer droplet into the elongated and intertwined fibers, forming rope-shaped e-spin nanomaterials.

Tissues with tubular structures, such as blood vessels, trachea, lymph vessels, and intestines were abundant in the bodies of the higher animals [221,222]. And various types of biocompatible tubular materials were fabricated via e-spin, in which the manipulation of the electric field and the design of 3D collectors were crucial for the preparation of tube-shaped e-spin nanomaterials [214,223,224]. For instance, tubular nanomaterials with the interconnected tubular passage were fabricated using a 3D columnar collector [199]. The columnar collector was used to collect the e-spin fibers, followed with the removal of the collector (Fig. 10B). Similarly, double-layered tubular e-spin scaffold was prepared using a cylindrical collector. The inner layer was composed of chitosan hydrogel loaded with growth factor, and the outer layer was composed of polymer fibers loaded with growth factor (Fig. 2-Tube) [225]. Moreover, a multilayered e-spin scaffold in 1.5-mm diameter was developed using this strategy [226]. In addition, stress-induced rolling technology (SIRT) was a simple way to prepare 3D tubular structures [220,227]. Specifically, the 2D polymer layer was stretched, and then the polymer layer was rolled up into the 3D tubes with the ends closed (Fig. 10C).

### 3. Biological applications

The variety of topologies of the e-spin nanomaterials enabled a myriad of biological applications [6], such as tissue engineering, wound healing, drug/bioactive molecules delivery, diagnosis and biomimetics. According to the publication analysis, more than 50% biological applications of the e-spin nanomaterials lied in tissue engineering, because e-spin nanomaterials possessed the most important features existing in natural ECM [228,229]. E-spin nanomaterials were used to mimic or replace the architectures of complex biological tissues [230,231]. Moreover, e-spin nanomaterials were capable of absorbing excess exudates around the

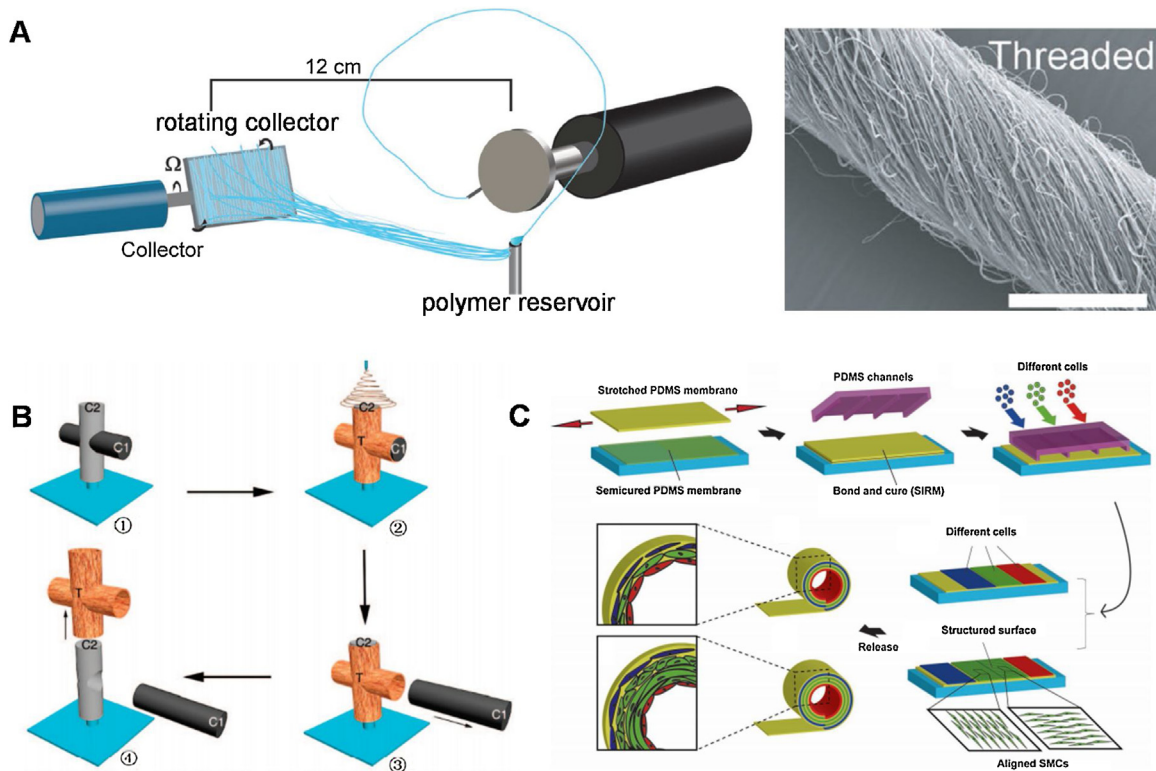


**Fig. 10.** Schematic illustration for the preparation strategies of rope and tube structures. (A) The manufacturing platform composed of a polymer reservoir and rotating collector was designed [219]; (B) Tube-shaped e-spin nanomaterials with the interconnected tubular passage [199]; (C) 3D electrospun tubes seeded with cells were fabricated via stress-induced rolling technology. The 2D fibrous mats were rolled into the 3D tubes using this technology [220]. Sources: [219,220], Copyright 2017, 2012, respectively. Reproduced with permission from Wiley-VCH; [199], Copyright 2008. Reproduced with permission from the American Chemical Society.

wounds and promoting the exchanges of airflow, offering comfortable surface environments for cell growth and finally achieving “perfect repair” [232–235]. The surface patterns of e-spin nanomaterials with radially aligned features were highly desired for wound healing [236]. E-spin nanomaterials were used to deliver various classes of bioactive molecules and drugs, due to their high specific surface area, desirable topologies for release kinetics, great flexibility in selecting carrier materials and molecular-level alignments [237,238]. E-spin nanomaterials exhibited huge potential for intensifying the specificity, sensitivity and signaling capabilities of miscellaneous biomarkers in human disease [5,239–241]. In addition, e-spin was regarded as the one of the most excellent technologies to construct biomimetic structures [19].

Surface functionality and topologies of e-spin nanomaterials played important roles in biological applications [243]. A variety of bioactive components and chemical groups were grafted onto the surface of e-spin nanomaterials through chemical or physical interactions, such as proteins [244,245], peptides [246,247], aptamers [245], collagen [248], calcium and orthophosphate ions [249], growth factor [226,250], antibiotics [251], anticancer drugs [252], nitric oxide (NO) [253], RNA [128,139,254], viral gene [124], non-viral gene [135], and plasmid DNA [255]. The surface functionalized e-spin nanomaterials had great impacts on the related biological applications via regulating the cellular metabolism and signaling pathway [27,256,257]. For instance, when the surface chemical groups of e-spin fibers changed from isocyanate (NCO) groups to amino groups, the hydrophilicity of fibers was enhanced, and the non-specific protein adsorption was suppressed (Fig. 11A&B) [242]. Moreover, the covalent attachment of RGD peptide (promote cell adhesion) on the surface of fibers promoted cell adhesion and differentiation, controlling cell behavior and metabolic activi-

ity (Fig. 11C). Furthermore, a variety of chemical groups were covalently attached to the surface of the e-spin fibers using click chemistry, such as alkyne, tyrosine – phenol, ketone, alkene and azide groups [258]. Considerable excellent reviews have summarized the biological applications of the e-spin nanomaterials and stressed the importance of surface functionality on biological applications [5,42,214,259–261], and we herein put our emphasis on the correlation between the topologies of e-spin nanomaterials and their biological functions and applications.

### 3.1. Tissue engineering

Damage of many tissues in the human body is irreversible and unable to repair itself [262]. Even with the surgical intervention, recovery of function is often limited, and the healing response is scar-mediated rather than regenerative. Grafts (scaffolds) used in surgery have some limitations which restrict their extensive applications, such as short self-life, high cost, and poor mechanical properties to withstand handling [263]. Therefore, designing and fabricating new grafts is important [264]. An ideal scaffold should satisfy the following requirements: 1) favorable biocompatibility and admirable mechanical property; 2) desirable topologies allowing for cell ingrowth and mass transport of nutrients, oxygen, and waste products [259,265]. The topologies of e-spin nanomaterials were similar to the interwoven protein fibers in tissues, showing great potential for tissue regeneration [266].

On account of the diversity of topologies, e-spin nanomaterials with different topologies were designed and fabricated for tissue engineering. Cell behavior was regulated by changing the surface morphology of individual fibers. When hippocampal neuron cells were cultured on smooth fibers, the cells only distributed on the fiber grooves, and primary neurites without orientation were

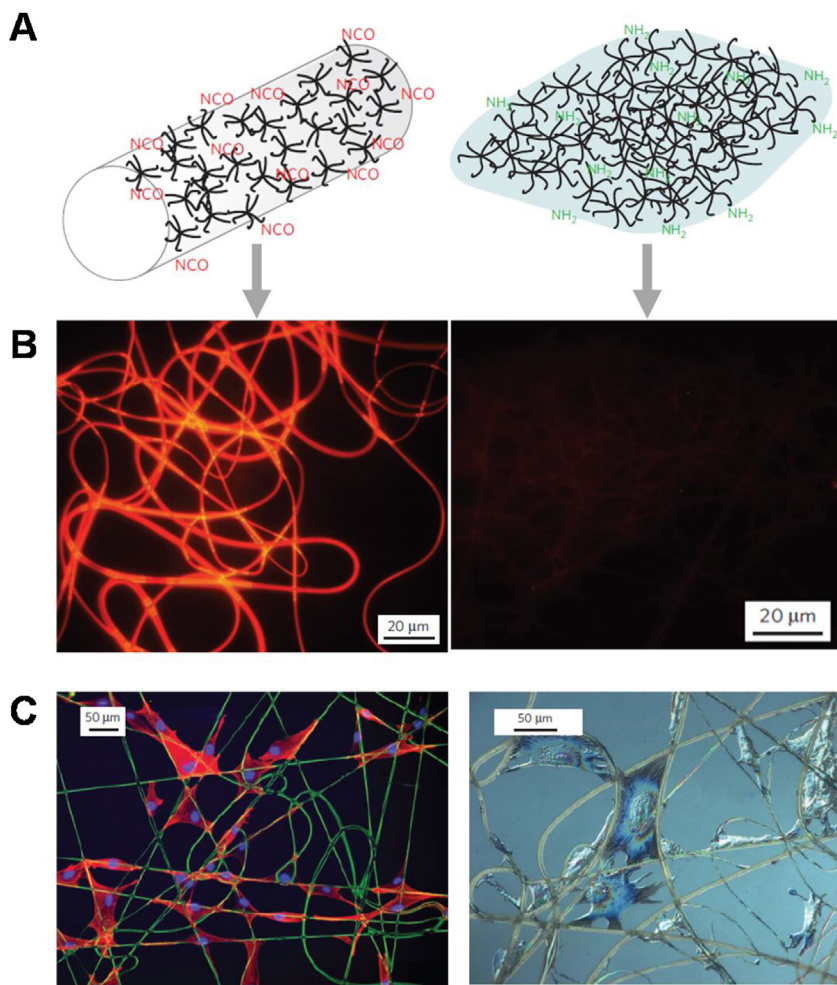


**Fig. 11.** Surface functionality. (A) Scheme for the covalent attachment of two different chemical groups on the e-spin fibers. Isocyanate (NCO) groups: red; amino groups: green. (B) Fluorescence images of the protein (red) absorbed on the surface of fibers. (C) Fluorescence and optical images of human dermal fibroblasts (nuclei blue, actin filaments red) after culturing with RGDS (a kind of peptide for promoting cell adhesion)-functionalized e-spin fibers [242], Copyright 2011. Reproduced with permission from the Nature Publishing Group.

observed (Fig. 12A) [267]. When neuron cells were cultured on microcages with multi-channels and different widths, cells not only distributed on the grooves, but also elongated the cellular processes in the breaking points and grooves, showing high orientation of neuron cells (Fig. 12B) [267]. Regarding *Hybrids*, cell behavior and metabolism were regulated via introducing bioactive components. For example, VEGF and PDGF were incorporated into e-spin fibers, which promoted endothelialization, and inhibited smooth muscle cells hyperproliferation (Fig. 12C) [226]. Moreover, the fibrous vascular scaffold loading with growth factors were utilized to maintain patency in rabbit carotid artery for 8 weeks. Besides, multiple cells were incorporated in e-spin fibers by directly seeding cells on the surface of fibers [220].

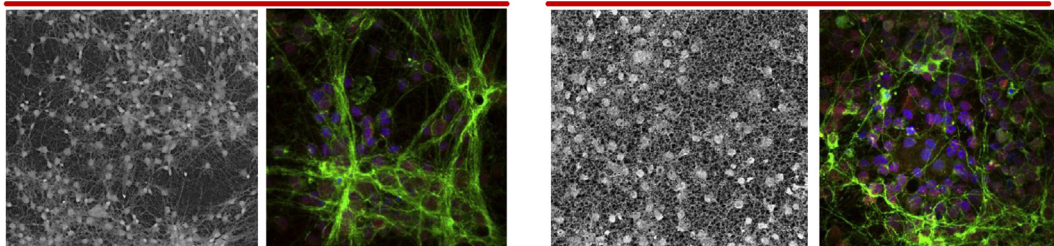
Regarding *Assemblies*, cell behavior was regulated by changing the 3D topologies of e-spin nanomaterials. When the cells were seeded on the surface of non-woven mats, the cell behavior was adjusted via changing the stiffness of the attached fibers [268]. As the fiber stiffness was increased, cell proliferation and spreading were suppressed. Specifically, when the cells were attached on soft fibers, cells recruited nearby fibers and promoted to form focal adhesions and enhance cell signal transduction (Fig. 12D). When the nerve stem cells were incorporated into the aligned e-spin fibers, the anisotropic morphology of aligned fibers guided and promoted the outgrowth of neuritis [269]. Cells tended to attach parallel on aligned nanofibers (Fig. 12E). Moreover, the ani-

mal experiments indicated that the length of neurites cultured on aligned fibers were larger than that of non-woven fibers [270]. On the helical fibers, human mesenchymal stem cells (hMSCs) were easily penetrated into the interior of the helical fibers; however, milder myofibroblastic differentiation was observed (Fig. 12F) [188]. In contrast, non-woven fibers induced hMSCs to differentiate into fibroblast phenotype through regulating the expression of related genes and proteins, resulting in the dense distributions of cells, due to the limited cell infiltration in non-woven fibers.

Crimping structures were similar to that of the native anterior cruciate ligament [271]. When the bovine fibroblasts were seeded on the surface of crimping fibers, cells were easily attached to the fiber, causing significant cell proliferation and collagen deposition (Fig. 13A). Notably, one major limitation of the e-spin nanomaterials for tissue engineering was the dense fiber distribution with small pore size, causing poor cell infiltration [93]. Patterned e-spin nanomaterials were able to adjust the distribution and size of fibers to promote endothelial cells ingrowth and increase M2 macrophage (Fig. 13B). The elastic modulus of patterned nanomaterials decreased with the increase of the hole size, indicating the adjustable mechanical property. Cells seeded on different patterned nanomaterials exhibited different cell distributions but similar cell proliferation rate. In addition, cell adhesion and orientation were regulated via choosing appropriate patterned

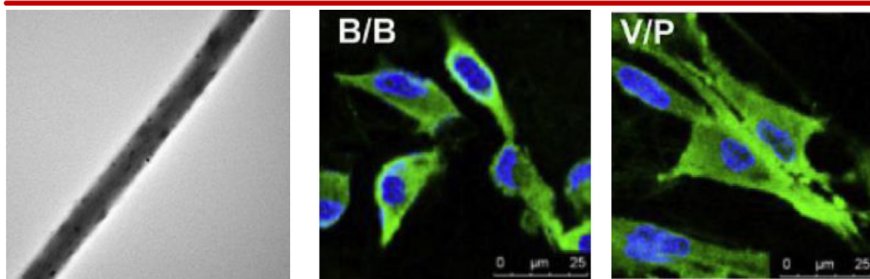
## INDIVIDUALS

### A Fiber



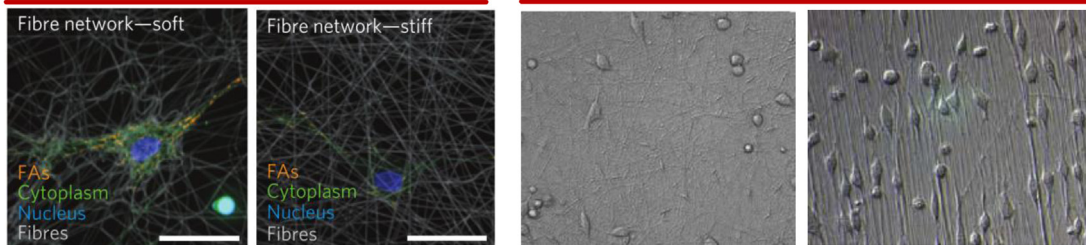
## HYBRIDS

### C Bioactive molecules

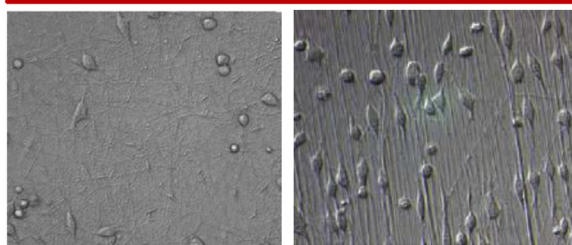


## ASSEMBLIES

### D Non-woven



### E Aligned array



### F Helical

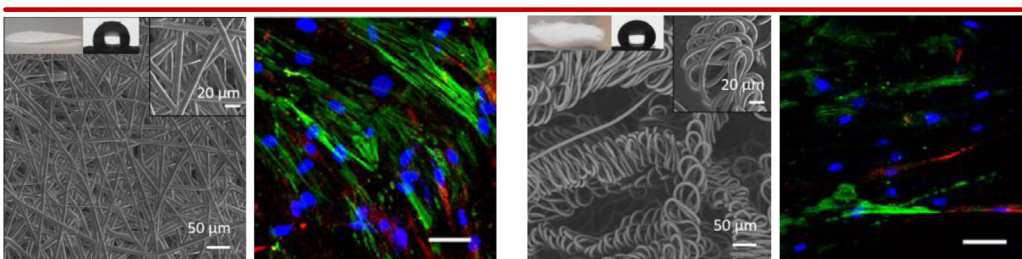


**Fig. 12.** Tissue engineering. (A&B) SEM and laser confocal images of hippocampal neurons after culturing on the e-spin nanomaterials. Cells were stained for βIII-tubulin (green), GAP43 protein (red, positively correlated with axonal outgrowth) and nuclei (blue). A: smooth fibers; B: microcages [267]; (C) Left: TEM images of the e-spin fibers containing vascular endothelial growth factor (VEGF) and platelet-derived growth factor-bb (PDGF); middle and right: laser confocal images of vascular smooth muscle cells (VSMCs) cultured with different bioactive e-spin fibers. (B: blank, V: VEGF, P: PDGF, smMHC-I protein green, nuclei blue) [226]; (D) Fluorescence images of the F-actin (FAs) formation on non-woven mats composed of low and high fiber stiffness (FAs orange, cytoplasm green, nuclei blue and fiber grey) [268]; (E) Phase contrast light images of neural stem cells attachment on aligned fibers and non-woven fibers [269]; (F) SEM and confocal images of non-woven and helical fibers cultured with human mesenchymal stem cells (hMSCs). Nucleus: blue; FSP1 (fibroblastic phenotype): red; α-SMAs (α-smooth muscle actin): green [188]. Sources: [226,267,269], Copyright 2013, 2010, 2005, respectively. Reproduced with permission from Elsevier Ltd; [268], Copyright 2015. Reproduced with permission from the Nature Publishing Group; [188], Copyright 2016. Reproduced with permission from the American Chemical Society.

shapes and directions [200,204]. Moreover, e-spin nanomaterials with complex patterning structures were used to regulate the cell morphology and distribution at the same time [206]. The cell morphology was regulated through changing the patterned dimensions, while the cell distribution was regulated via designing the patterned orientation (Fig. 13C). Thus, the complex patterning structures were able to achieve the cell distribution with complexity and anisotropy in the same sample, demonstrating the great

potential for designing multifunctional tissue scaffolds. Rope and tube with micron scaled features showed variations even within the same sample, which was designed to regulate the variety of cellular interactions and complex biochemical reactions [272–274]. Rope structures were able to promote the muscle cell proliferation and differentiation, due to the highly anisotropic fiber structures [219]. The cells were attached on the fibers along the fiber axis, exhibiting the extended morphologies (Fig. 13D). In addition, mul-

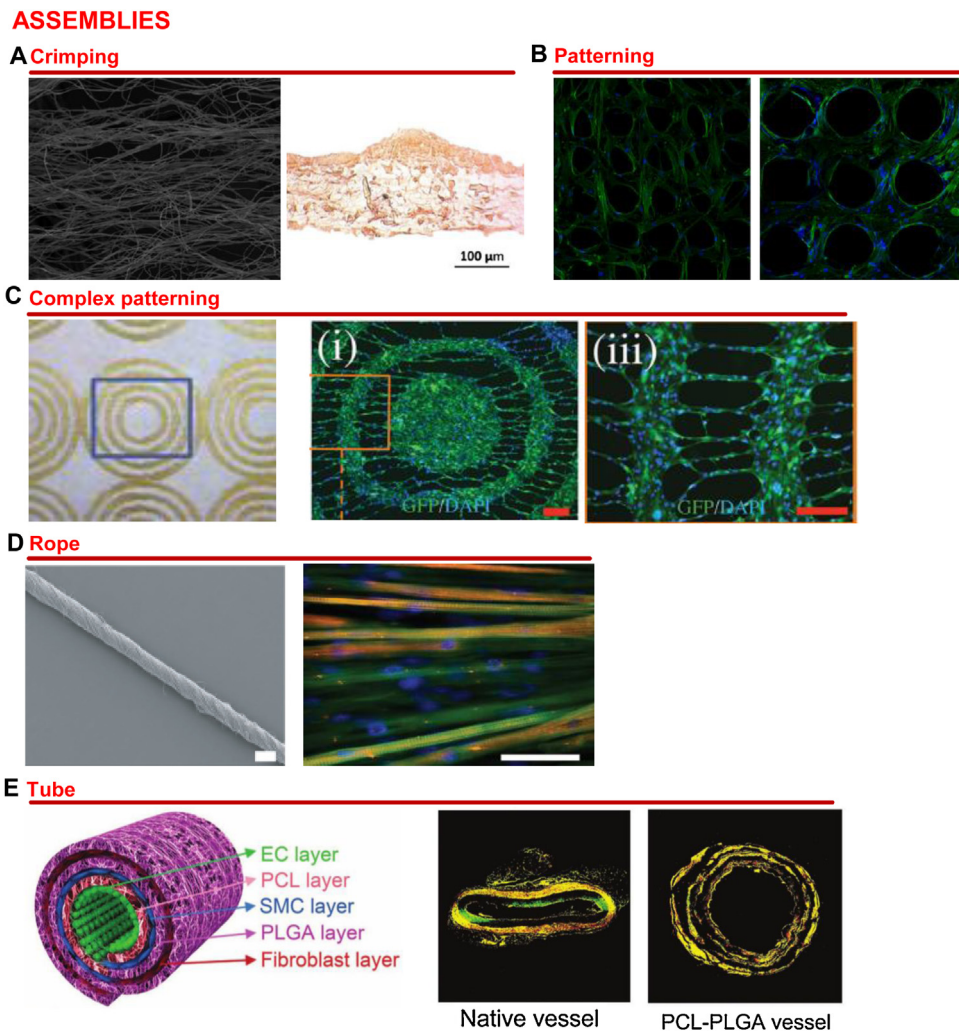


**Fig. 13.** Tissue engineering. (A) Left: SEM images of the crimping fibers; right: picrosirius red staining histology images of the crimping fibers attached to ligament tissues [271]; (B) Fluorescence images of hMSCs seeded on the surface of different patterned e-spin nanomaterials. Actin: green; cell nucleus: blue [93]; (C) Left: the AutoCAD patterns of the concentric circle; right: fluorescence images of the cells cultured with the corresponding patterned nanomaterials [206]; (D) Left: SEM images of rope-shaped fibers; right: immunofluorescence image of murine skeletal muscle cultured with the rope-shaped fibers. Nuclei: blue; F-actin: green;  $\alpha$ -actinin: red [219]; (E) Left: Scheme for poly(ε-caprolactone)-poly(DL-lactide-co-glycolide) (PCL-PLGA) tube with three kinds of related cells distributed in different layers; right: immunofluorescent images of native vessel and PCL-PLGA tubes staining with CD 31 (red), collagen I (red), and collagen III (green) [275]. Sources: [93,271]. Copyright 2012. Reproduced with permission from Elsevier Ltd; [206,219,275]. Copyright 2014, 2017, 2017, respectively. Reproduced with permission from Wiley-VCH.

tilayered and blood vessel-mimicking e-spin nanomaterials with controlled biodegradation rate were developed as the vascular stent [275]. Three types of cells were seeded on different layers of the tube through mimicking the distribution of cells in blood vessels. When the tube was implanted in rabbits, the inner layer expanded, while the outer layer shrank, maintaining the structural stability of the tube with enhanced cell infiltration and growth. Immunofluorescent analysis indicated that structural remodeling of the tube-shaped nanomaterials was enhanced compared with native vessel due to the lower content of the collagen III (green, the major component of scar) (Fig. 13E). Notably, cells were able to sense the changes of external microenvironment [276]. When the cells were encapsulated in e-spin nanomaterials, the topologies of e-spin nanomaterials played critical roles in regulating the cell behavior [277]. Specifically, An et al. fabricated the patterned hydrogel composed of electrospun nanofibers for cell encapsulation, and the patterned fibrous structures were utilized to adjust mass transfer and promote cell loading. Moreover, the cell encapsulation using nanofiber-based devices was an important area of biological application and had great potential for inducing cells oriented differentiation and therapies [278].

### 3.2. Wound healing

Every year, more than 6 million patients suffered from severe burns and over 300,000 people ultimately died from these injuries worldwide [279,280]. Wound dressing offered protective barrier to assist in many aspects of the healing process [281]. An ideal wound dressing not only protected the wound from microbial infection, allowed gas exchange, absorbed excess exudates, but also maintained a moist environment to enhance epithelial regrowth, and be painless to remove [282]. E-spin nanomaterials possessing high specific surface area, adjustable porosity and controlled topologies promoted related cell proliferation and tissue regeneration. Through introducing bioactive components related to wound healing, bio-functionalized e-spin nanomaterials were fabricated to achieve “perfect healing” via regulating the related metabolic pathway and growth factors [283]. For instance, TGF $\beta$  was an important growth factor to control and regulate variety of cellular functions, which was closely related to the wound healing process. In different cellular contexts, various TGF $\beta$  subtypes including TGF $\beta_1$ , TGF $\beta_2$ , TGF $\beta_3$ , and TGF $\beta_4$  played important roles in almost all stages of wound healing and scar formation [284]. Notably, TGF $\beta_1$ /Smad sig-

naling pathway was utilized to promote wound healing through designing nanomaterials with bio-functions and specific topology [285].

Topologies of e-spin nanomaterials exhibited influences on the process of wound healing. Through designing appropriate topologies, the surface bio-functionality, matrix degradation rate and surface chemistry were tuned to govern the materials–biology interfacial interactions. Regarding *Individuals*, smooth fibers were used to adjust the biomechanics and promote the wound healing [286]. For instance, gelatin fibers were crosslinked to increase the fiber density and mechanical strength, causing the increased deposition of collagen (Fig. 14A). And the high expression of the specific collagen indicated the optimal wound healing process. Further, porous e-spin nanomaterials were favor to the respiration of cells, providing an appropriate moist environment for the wound [290]. The small pore size effectively protected the wound from bacterial infection. With regard to *Hybrids*, incorporating exogenous components related to the wound repair accelerated the process of wound healing. A variety of non-bioactive and bioactive components were incorporated into e-spin nanomaterials to promote tissue regeneration, inhibiting infections and accelerating the wound healing, such as metal–organic frameworks (MOFs) [291], zinc oxide nanorods [292], silver nanoparticles [293], type I collagen monomer [294], nitric oxide [295], antimicrobial peptide [296], ostholamide [297], and phenytoin [298]. For example, PCL e-spin nanomaterials incorporated with silver nanoparticles were prepared to achieve long-term broad-spectrum antimicrobial activity [287]. The *in vivo* studies revealed that the e-spin nanomaterials reduced the inflammatory response and achieved a perfect postoperative outcome (Fig. 14B). Moreover, rapid hemostasis was achieved in a few seconds by depositing the e-spin nanomaterials on the surface of the wound. Drugs such as curcumin mobilized the fibroblasts to promote wound healing via activating the WNT signaling pathway [288]. E-spin nanomaterials with curcumin enhanced the bioavailability of curcumin and promoted migration of skin cells to achieve self-repair (Fig. 14C). Bioactive molecules such as NO were utilized to promote granulation formation and re-epithelialization, improving the regenerated tissues and achieving perfect healing [289]. E-spin nanomaterials encapsulated with NO promoted the related collagen deposition, angiogenesis and immunomodulation (Fig. 14D). Synergetic effects were achieved via introducing non-bioactive and bioactive components simultaneously. For example, nanoparticles-in-nanofibers (NPs-in-NFs) wound dressings loaded with phenytoin achieved remarkable re-epithelialization with minimal necrotic cells formation and inflammation [298]. Regarding *Assemblies*, cell migration and endothelialization were regulated and enhanced by changing the arrangements of fibers. The aligned array fibers enhanced cell migration from the periphery to the center of the wound, while the non-woven fibers were not able to accelerate the process of wound healing (Fig. 14E and F) [236]. And the arrangement of collagen deposition was similar to that of natural extracellular matrix, when the aligned array fibers were used. Besides, non-woven fibers with the controllable distribution of nano-porous architectures were used to induce the cell migration to the surface of the wound [299].

### 3.3. Drug/bioactive molecules delivery

The limitations of current drug/bioactive molecules delivery systems include limited targeted efficiency, potential cytotoxicity and suboptimal bioavailability [300]. E-spin was regarded as the one of most suitable candidates to achieve the controlled release of drug/bioactive molecules, due to controllable diameters and compositions, flexibility in selecting materials, desirable topologies, high specific surface area and easy processing [301,302]. Notably,

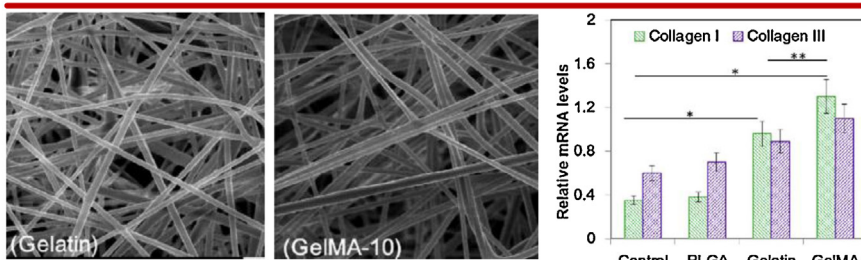
the release kinetics, loading capacity and biocompatibility of the drug/bioactive molecules were able to be regulated via changing the topologies of e-spin nanomaterials.

On account of the controllability of topologies, some topologies favored drug/bioactive molecules delivery. Regarding *Individuals*, adjusting the pore distributions of e-spin nanomaterials regulated the release kinetics of the payloads effectively. For instance, emulsion e-spin was utilized to fabricate hollow nanomaterials to load QK peptide (promoting the growth of vascular endothelial cells) [303]. *in vitro* cell culture experiments indicated that the release of QK peptide accelerated the proliferation of vascular endothelial cells (Fig. 15A). Compared with smooth fibers, the release rate of hollow fibers was significantly reduced to achieve a long-term sustained release. Similarly, Huang et al. fabricated double-layered hollow fibers to hinder the initial burst release of the payloads, achieving the sustained release manner without destroying their physiological activity [310]. In order to further reduce the release rate of individual fibers, core-shell fibers were prepared using liposome as the new barrier (Fig. 15B) [304]. The structure of core-shell fibers provided two barriers for the release of drugs/bioactive molecules, achieving a more controllable manner. Further, highly porous e-spin nanomaterials were able to achieve high drugs loading, overcome mass transfer limitations, and build new pathways for fluid transportation [311]. For instance, porous fibers were used to capture and nondestructively release the specific circulating tumor cells [312]. In order to control the release manner of porous fibers, air served as the barrier component was developed [305]. For example, porous fibers with entrapped air layer prolonged the release of the cancer cells *in vitro* for more than 2 months (Fig. 15C). And the release rate of porous fibers was accelerated via removing air around the fibers.

Regarding *Hybrids*, various types of non-bioactive/bioactive components were introduced into e-spin nanomaterials for the controlled release. On-demand release behavior was urgently required for drug/bioactive molecules delivery, such as controlled and stimuli-responsive release manners. For instance, nanoparticles loading with the payloads were introduced into the e-spin nanomaterials to achieve the controlled release manner [287]. Similarly, the introduction of chitosan nanoparticles containing siRNA into e-spin nanomaterials showed a controlled release fashion and exhibited a high gene silencing efficiency after two days [129,130]. Stimuli responsive e-spin nanofibers doped with mesoporous silica nanoparticles were developed to achieve on-demand and controlled release manner [306]. The release rate of the payloads was adjusted via changing the intensity and time of ultrasound irradiation. The release rate of the multi-payloads was different, due to the differences in the sensitivity to the ultrasound irradiation (Fig. 15D). Besides, the delivery of various drugs was a direct and simple way for the disease treatment. For instance, when e-spin nanomaterials encapsulated with dichloroacetate (anticancer drugs) were covered to the surface of solid tumor, the growth of the tumor was significantly suppressed, resulting in the dramatic decrease in volume and weight of the target tumors (96% of the tumor suppression degree) (Fig. 15E) [307]. In order to improve the treatment effect, multiple synergistic drugs were introduced into the e-spin nanomaterials. For example, rifampicin and fusidic acid co-loaded e-spin nanomaterials were developed for preventing postoperative infections [313]. Moreover, three drugs were incorporated into nanomaterials for bone regeneration [314]. In addition, bioactive molecules were potential candidates for the disease treatments. For instance, e-spin nanomaterials with siRNA genes were developed to suppress the formation of fibrous capsule by down-regulating the expression of collagen type I (Fig. 15F) [308]. Compared with conventional bolus delivery of siRNA, e-spin nanomaterials-mediated siRNA delivery prolonged the gene silencing duration by at least 2–3 times [315]. And the gene

## INDIVIDUALS

### A Fiber

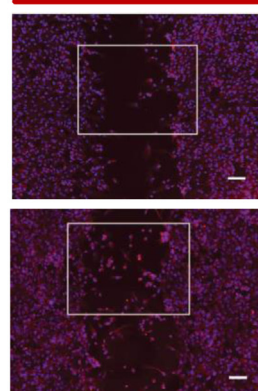


## HYBRIDS

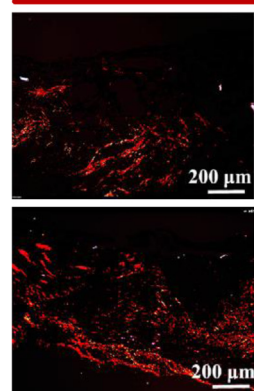
### B Nanoparticles



### C Drugs

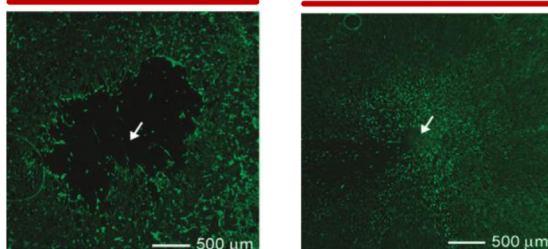


### D Bioactive molecules



## ASSEMBLIES

### E Non-woven



### F Aligned array

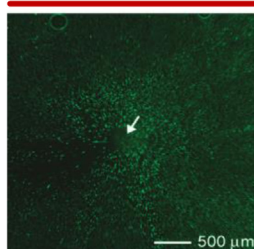


**Fig. 14.** Wound healing. (A) Left: SEM images of the smooth gelatin fibers with/without fiber crosslinking; right: qRT-PCR results of the relative mRNA levels, which were related to the contents of collagen deposition [286]; (B) Gross observation images of the skin wounds treated with gauze, polycaprolactone (PCL) mats, and silver nanoparticles doped PCL mats, respectively [287]; (C) Fluorescence images of fibroblast cell migration in a scratch test.  $\beta$ -catenin: red; nuclei: blue [288]; (D) Fluorescence images of the collagen deposition (red) with/without NO [289]; (E&F) Fluorescence images of the migration of fibroblast cells when the dura tissues were cultured with the non-woven (E) and aligned array fibers (F) for four days [236]. Sources: [286,289], Copyright 2017. Reproduced with permission from Elsevier Ltd; [287], Copyright 2016. Reproduced with permission from the Royal Society of Chemistry; [288], Copyright 2017. Reproduced with permission from the Nature Publishing Group; [236], Copyright 2011. Reproduced with permission from the American Chemical Society.

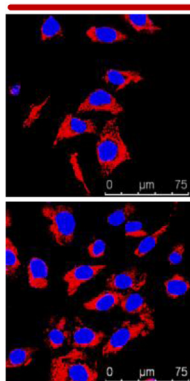
silencing duration was further prolonged by designing appropriate topologies [316]. For example, Cao et al. encapsulated siRNA within e-spin nanomaterials and achieved sustained release for at least 28 days [133]. With regard to *Assemblies*, preparing e-spin nanomaterials with appropriate 3D structures was the key parameter for drug/bioactive molecules delivery. Micron-sized and multi-compartmental hydrogels prepared by patterned e-spin nanomaterials were developed to achieve multiple drug/bioactive molecules release step by step [309]. In detail, sequential e-spin was utilized to produce multi-layered e-spin mats with different compositions. Then the mats were covered with precursor solution for hydrogel formation. The patterned hydrogel particles achieved multiple drugs/bioactive molecules release with independent kinetics simultaneously (Fig. 15G). In addition, tubular e-spin nanomaterials with two growth factors were developed to promote vascular endothelial cell proliferation and revascularization compared with the control group (Fig. 15H) [225].

### 3.4. Diagnosis

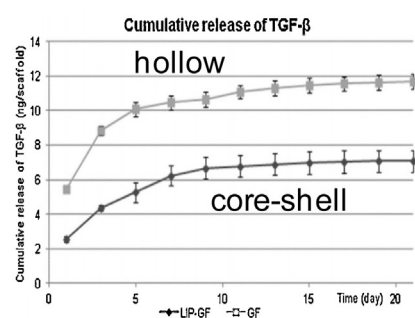
Medical diagnosis, especially the early diagnosis is very important for the treatment of diseases, such as cancers and rare diseases [317]. Taking lung cancer as an example, it is usually diagnosed in advanced stage when survival rate is very low, so the early diagnosis is of vital importance. The critical issues in the field of medical diagnosis are to improve the specificity, sensitivity and signaling capabilities of miscellaneous biomarkers in human diseases [318,319]. Polymer-based materials have been served as the indispensable matrix for the medical diagnosis, due to their multifunction, multiple-responsiveness and biocompatibility [317]. However, the detection limit of biomarkers is not satisfied for the practical applications directly using the polymer matrix without modifications. Thus, the combination of polymer-based e-spin nanomaterials with medical diagnostics exhibits great potential for targeting the practical problems of early medical diagnosis, due

## INDIVIDUALS

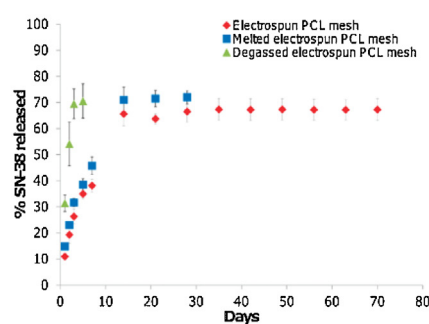
### A Hollow



### B Core-shell

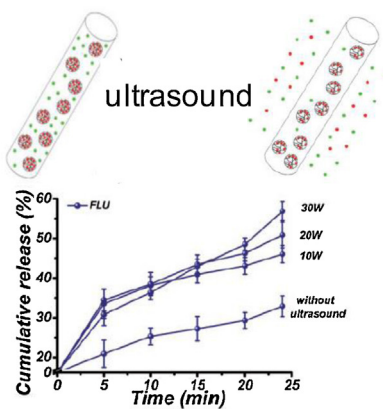


### C Porous

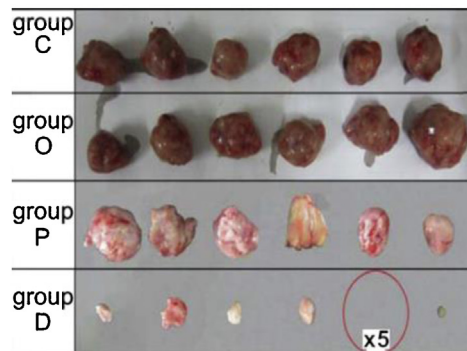


## HYBRIDS

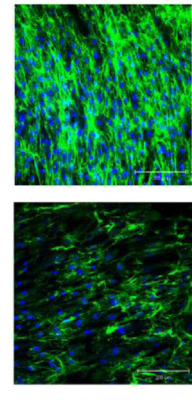
### D Nanoparticles



### E Drugs

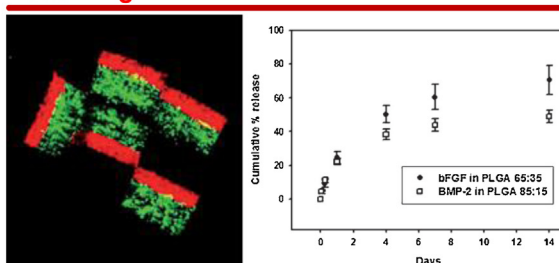


### F Bioactive molecules



## ASSEMBLIES

### G Patterning



### H Tube

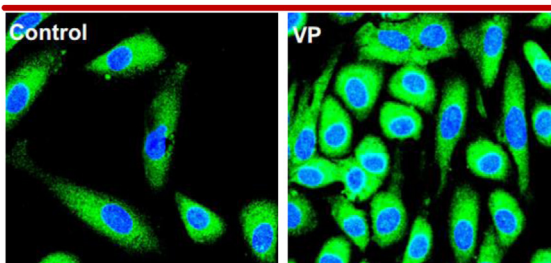


**Fig. 15.** Delivery of drug/bioactive molecules. (A) Immunofluorescence images of the human umbilical vein endothelial cells cultured with hollow fibers with (bottom)/without (top) QK peptide. Anti-CD31 antibody: red, nuclei: blue; (B) Cumulative release profile of the TGF- $\beta$  growth factor in hollow and core-shell fibers, respectively; (C) Release profiles of the SN-38 from native, melted and degassed porous fibers, respectively; (D) Top: scheme of the release process by applying the ultrasound irradiation; bottom: the release profiles of the payloads by applying ultrasound irradiation with different powers (10 W, 20 W, 30 W); (E) The digital photos of tumor growth and suppression using e-spin nanomaterials with dichloroacetate; (F) Fluorescence images of the target cells cultured with (bottom)/without (top) siRNA-loaded e-spin nanomaterials; (G) Left: fluorescence images of the bi-compartmental hydrogel patterned microparticles; right: bi-compartmental patterned microparticles for controlled release of two kinds of growth factors independently; (H) Immunofluorescence images of the vascular endothelial cells cultured on the surface of the tube-shape e-spin nanomaterials (anti-CD31 antibody: green; nuclei: blue). Sources: [303], Copyright 2016. Reproduced with permission from Springer-Nature; [304,305], Copyright 2012. Reproduced with permission from the American Chemical Society; [306], Copyright 2015. Reproduced with permission from Oxford University Press; [309], Copyright 2015. Reproduced with permission from Wiley-VCH; [225,307,308], Copyright 2017, 2012, 2013, respectively. Reproduced with permission from Elsevier Ltd.

to their high specific surface area, flexible topologies and surface chemistry. Through adjusting the topologies of e-spin nanomaterials, the detection specificity, sensitivity and signaling capabilities were enhanced [320,321].

Regarding *Individuals*, e-spin nanomaterials with high porosity and specific area were able to enhance the detection sensitivity [320]. Through incorporating the red fluorescent labeled anti-

body, acquired immune deficiency syndrome (AIDS) virus was only detected in HIV positive serum (Fig. 16A). Besides, the e-spin nanomaterials with core-shell structures were utilized to capture and release the specific cells from blood for the subsequent diagnosis and analysis of single cell [150]. In detail, temperature-responsive polymer named poly(N-isopropylacrylamide) was chosen to prepare core-shell e-spin nanomaterials, and the hydrophobicity of

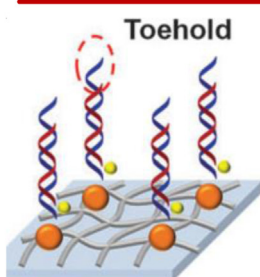
## INDIVIDUALS

### A Porous

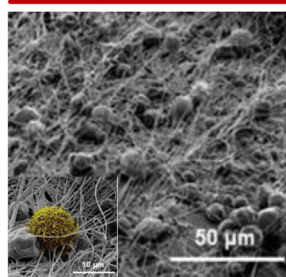


### HYBRIDS

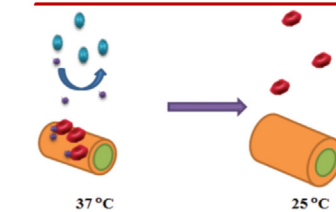
#### C Nanoparticles



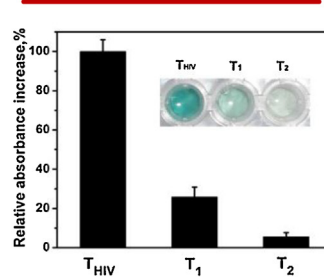
#### D Beads



### B Core-shell

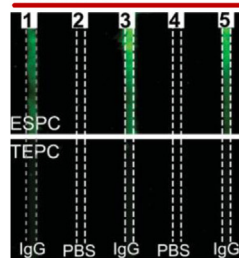


#### E Bioactive molecules



## ASSEMBLIES

### F Non-woven



### G Helical

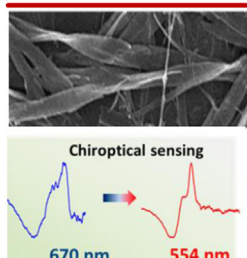


**Fig. 16.** Medical diagnosis. (A) Fluorescence images of porous e-spin nanomaterials exposed to HIV negative serum (left) and HIV positive serum (right); (B) Scheme of the process of capturing and releasing of red blood cells (RBCs) using temperature as a switch; (C) Scheme of the e-spin nanomaterials loading with DNA-functionalized gold nanoparticles for nucleic acid detection; (D) SEM images of beads doped e-spin nanomaterials for capturing the MCF7 cells; (E) Visual detection of the HIV virus using the multiple bioactive molecules doped e-spin nanomaterials. Inset photos showed the corresponding color change for detecting the virus; (F) The results of fluorescence intensity for detecting HIV virus using non-woven e-spin nanomaterials; (G) Helical fibers showed circular dichroism signals, utilized for medical diagnosis and sensing. Sources: [150,320,321], Copyright 2016, 2016, 2013, respectively. Reproduced with permission from the Royal Society of Chemistry; [322,324], Copyright 2015, 2008, respectively. Reproduced with permission from Wiley-VCH; [323], Copyright 2016. Reproduced with permission from the Nature Publishing Group; [325], Copyright 2016. Reproduced with permission from the American Chemical Society.

e-spin nanomaterials switched by changing temperature, enabling capture or release of the specific cells (Fig. 16B). The release efficiency reached to 100% without the destruction of cellular function. Regarding *Hybrids*, inorganic particles or bioactive components were incorporated into the e-spin nanomaterials to reduce the detection limit and achieve biosensing and imaging. For example, e-spin nanomaterials doped with DNA-functionalized gold nanoparticles were utilized for highly sensitive detection of breast cancer susceptibility gene (Fig. 16C) [321]. Similarly, nylon 6 nanofibers loaded with carbon nanotube were served as the enzyme electrocatalytic immunosensor for detecting tumor suppressor protein [326]. Further, microbeads doped e-spin nanomaterials provided a three dimensional fibrous interface to capture the rare number of cancer cells from the blood, due to the stereo trap effect [322]. The cell fitting microsized pores created by the microbeads in e-spin nanomaterials enabled the capture of cancer cells effectively (Fig. 16D). Besides, bioactive molecules were incorporated into the e-spin nanomaterials to further decrease the detection limit. For instance, branched DNA probe was introduced into the e-spin nanomaterials to amplify the fluorescence signal and the detection limit was decreased to 20 pM via taking advantage of the dual-amplification effects of the strong fluorescence intensity

of branched DNA probe and the high surface area-to-volume ratio of e-spin nanofibers [326]. Moreover, multiple bioactive molecules including glucose oxidase, DNAzyme, DNA hairpin were introduced into e-spin nanomaterials to achieve visual detection of HIV biomarkers combining different bio-based amplification reactions [323]. The target nucleic acid analysis was detected and visualized by directly using naked eyes (Fig. 16E). Regarding *Assemblies*, multiple 3D topologies of e-spin nanomaterials were used for biosensing and visual detection. For instance, non-woven e-spin nanomaterials immobilized with antigens were fabricated for HIV diagnosis [324]. The results indicated that e-spin nanomaterials improved the sensitivity of detection, which was significantly better than that of the commercial rack-etched polycarbonate (TEPC) (Fig. 16F). Further, microchip on e-spin mats enabled on-site diagnosis of antigens, and the adsorption capacity of antigens was eight times more than that of TEPC [327]. With regard to detecting cells, non-woven e-spin nanomaterials achieved clinical diagnosis of the colorectal cancer via capturing the extremely low amounts of circulating tumor cells [328]. Due to chiral characteristics of the helical fibers, helical structures showed great potential for medical diagnosis and sensing by using circular dichroism as a detection signal readout (Fig. 16G) [325].

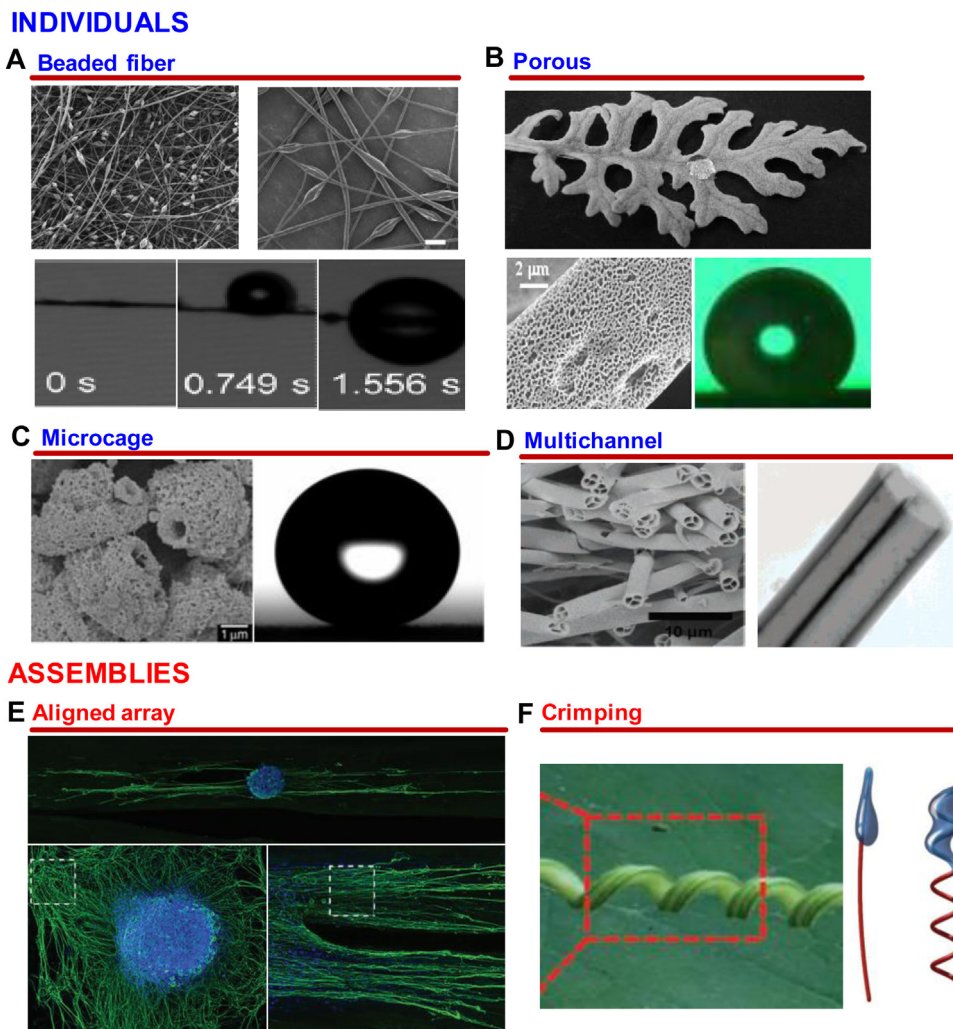


**Fig. 17.** Biomimetics. (A) SEM images of beaded fibers (top); fog-collection experiments on the beaded fiber at different time (bottom); (B) Digital photos of the hydrophobic silver ragwort leaf (top); SEM images of the porous polystyrene (PS) fibers and the water droplet dropped on PS; (C) SEM images of the polystyrene-based microcages (left), and the water droplet dropped on the surface of microcages; (D) TEM and SEM images of the e-spin nanomaterials with multichannel structures; (E) Fluorescence images of the rat dorsal root ganglion (DRG) neurite outgrowth cultured with the aligned array fibers. Anti- $\beta$ -tubulin III was stained green, and the nuclei was stained blue; (F) Digital photos of the coiled plant tendril (left); scheme of the adsorption of the crude oil using the crimping fibers. Sources: [343,345,347], Copyright 2012, 2004, 2017, respectively. Reproduced with permission from Wiley-VCH; [344], Copyright 2006. Reproduced with permission from IOP Publishing Ltd; [65], Copyright 2007. Reproduced with permission from the American Chemical Society; [346], Copyright 2016. Reproduced with permission from the Royal Society of Chemistry.

### 3.5. Biomimetics

Over millions of years of evolution, a large number of organisms possess fascinating structures, properties and functions, so that the preparation of biomimetic materials has become an increasingly important research field [329–337]. Inspired by Nature, biomimetics was thought to be a simple and practical method to fabricate multifunctional materials [338]. As a versatile and cost-effective nanofabrication technology, e-spin was regarded as the one of the most excellent technologies to construct a variety of biomimetic structures, such as lotus, water strider legs and Morpho butterfly [34,332,336,339–342].

Regarding *Individuals*, considerable biomimetic structures were fabricated by changing the surface/interior structure of the individual e-spin nanomaterials. Inspired by desert beetles, beaded fibers were prepared through adjusting the e-spin parameters [343]. The obtained beaded fibers collected water effectively, and the amount of water increased along with the time, exhibiting great potential for relieving the drought (Fig. 17A). Inspired by the structures of spider silk, beaded fibers were fabricated to respond to the environmental wetting [348]. Inspired by the self-cleaning properties

of silver ragwort leaf, super-hydrophobic porous e-spin nanomaterials were prepared, and the nanopores located on the surface of e-spin nanomaterials were demonstrated to be critical to regulate the hydrophobicity (Fig. 17B) [344]. Further, polystyrene-based e-spin nanomaterials with microcage structures showed super-hydrophobicity through mimicking the structure of lotus leaves (Fig. 17C) [345]. Inspired by the structure of the bird's feathers, e-spin nanomaterials with multichannel structures were prepared using multifluidic e-spin equipped with a modified spinneret (Fig. 17D) [65]. Regarding *Assemblies*, 3D biomimetic materials were fabricated. The ultimate goal was to reconstruct the cellular microenvironment that processed a wide range of signals such as physical, chemical, and mechanical cues, achieving perfect imitation of tissue structure [43]. Inspired by mussel adhesive chemistry, polydopamine-based non-woven e-spin nanomaterials were prepared to mimic the structure of bone [349]. As natural ECM degraded via the presence of matrix metalloproteinases, non-woven e-spin nanomaterials were developed to mimic the property of ECM and achieve protease-degradable property [350]. In contrast with non-woven fibers, hierarchically aligned e-spin nanomaterials cultured with nerve cells mimicked the oriented features of the

nerve tissue, providing biophysical cues to instruct cell behavior and fate (Fig. 17E) [346]. Considering the crimping structures of tendon tissue, crimping e-spin nanomaterials attached to the muscles or bones were developed to buffer mechanical loads, replacing the natural tendon tissue [197]. In addition, inspired by coiled plant tendril, crimping fibers were fabricated to adsorb the crude oil, because the crimping structure absorbed more components than the straight counterparts (Fig. 17F) [347].

#### 4. Conclusion and outlook

In this review, we summarize the topologies of e-spin nanomaterials that have been achieved in last decades and sketch a “topology periodic table”, providing a reference for scientists or engineers to opt for specific topology with desirable functions, as well as corresponding fabrication strategy. The topologies of e-spin nanomaterials are divided into three categories: *Individuals*, *Hybrids* and *Assemblies*, according to the intrinsic logical relationships. State-of-the-art progress on e-spin nanomaterials together with biological applications is comprehensively summarized. A considerable quantity of works have demonstrated that e-spin nanomaterials have high potential to solve the practical problems in biological applications, including tissue engineering, wound healing, drug/bioactive molecules delivery, medical diagnosis and biomimetics. Nevertheless, there still remain challenges in both fabrications and applications of e-spin nanomaterials.

- 1) Scale-up. Although there are already some e-spin industrial products such as e-spin nonwoven membrane, most of the materials with specific topologies are still prepared at a laboratory scale. Thus, scale-up fabrication strategies are required to cater for commercial and real-world applications.
- 2) Uniformity. Fabricating e-spin nanomaterials with high and uniform quality remains key challenging until now, as good biological performances strongly depend on the uniformity of materials.
- 3) Biological aspects. Although e-spin nanomaterials have been proved as potential candidates for biological applications, some issues still exist and need to be addressed. For example, allograft rejection, shrinkage, bulking or adsorption *in vivo* systems and the lower rate of migration of cells into e-spin nanomaterials are detrimental to the biological applications.
- 4) Multidisciplinary integration. At present, exploring on the deep integration between e-spin and other biological technologies is still not enough to meet diverse requirements of biological applications. This grand challenge needs the collaboration between researchers from multidiscipline.

#### Acknowledgements

This work was supported in part by National Natural Science Foundation of China (Grant No.: 21575101, 21622404, 21621004 and 51473118). We thank Dr. Feng Li for her kind and careful proofreading.

#### References

- [1] Whitesides GM. The ‘right’ size in nanobiotechnology. *Nat Biotechnol* 2003;21:1161–5.
- [2] Xia YN. Nanomaterials at work in biomedical research. *Nat Mater* 2008;7:758–60.
- [3] Roduner E. Size matters: why nanomaterials are different. *Chem Soc Rev* 2006;35:583–92.
- [4] Zhang L, Webster TJ. Nanotechnology and nanomaterials: promises for improved tissue regeneration. *Nano Today* 2009;4:66–80.
- [5] Sridhar R, Lakshminarayanan R, Madhaiyan K, Amutha BV, Lim KH, Ramakrishna S. Electrosprayed nanoparticles and electrospun nanofibers based on natural materials: applications in tissue regeneration, drug delivery and pharmaceuticals. *Chem Soc Rev* 2015;44:790–814.
- [6] Lu W, Sun J, Jiang X. Recent advances in electrospinning technology and biomedical applications of electrospun fibers. *J Mater Chem B* 2014;2:2369–80.
- [7] Shi JJ, Votruba AR, Farokhzad OC, Langer R. Nanotechnology in drug delivery and tissue engineering: from discovery to applications. *Nano Lett* 2010;10:3223–30.
- [8] Ramakrishna S, Fujihara K, Teo WE, Yong T, Ma Z, Ramaseshan R. Electrospun nanofibers: solving global issues. *Mater Today* 2006;9:40–50.
- [9] Agarwal S, Wendorff JH, Greiner A. Use of electrospinning technique for biomedical applications. *Polymer* 2008;49:5603–21.
- [10] Persano L, Camposeo A, Tekmen C, Pisignano D. Industrial upscaling of electrospinning and applications of polymer nanofibers: a review. *Macromol Mater Eng* 2013;298:504–20.
- [11] Bhattachari N, Li Z, Gunn J, Leung M, Cooper A, Edmondson D, et al. Natural-synthetic polyblend nanofibers for biomedical applications. *Adv Mater* 2010;21:2792–7.
- [12] Lu X, Wang C, Wei Y. One-dimensional composite nanomaterials: synthesis by electrospinning and their applications. *Small* 2009;5:2349–70.
- [13] Badrossamay MR, Mcilwee HA, Goss JA, Parker KK. Nanofiber assembly by rotary jet-spinning. *Nano Lett* 2010;10:12257–61.
- [14] Sarkar K, Gomez C, Zambrano S, Ramirez M, Hoyos ED, Vasquez H, et al. Electrospinning to forcespinning. *Mater Today* 2010;13:12–4.
- [15] Xu C, Wang L, Wang R, Wang K, Zhang Y, Tian F, et al. Nanotubular mesoporous bimetallic nanostructures with enhanced electrocatalytic performance. *Adv Mater* 2009;21:2165–9.
- [16] Lee TW, Byun Y, Koo BW, Kang IN, Lyu YY, Lee CH, et al. All-solution-Processed n-Type organic transistors using a spinning metal process. *Adv Mater* 2005;17:2180–4.
- [17] Jiang KL, Li QQ, Fan SS. Nanotechnology: spinning continuous carbon nanotube yarns. *Nature* 2002;419:801.
- [18] Dzenis Y. Spinning continuous fibers for nanotechnology. *Science* 2004;304:1917–9.
- [19] Li D, Xia Y. Electrospinning of Nanofibers: Reinventing the Wheel? *Adv Mater* 2004;16:1151–70.
- [20] Greiner A, Wendorff JH. Electrospinning: a fascinating method for the preparation of ultrathin fibres. *Angew Chem Int Ed* 2007;46:5670–703.
- [21] Ramakrishna S, Jose R, Archana PS, Nair AS, Balamurugan R, Venugopal J, et al. Science and engineering of electrospun nanofibers for advances in clean energy, water filtration, and regenerative medicine. *J Mater Sci* 2010;45:6283–312.
- [22] Agarwal S, Greiner A, Wendorff JH. Functional materials by electrospinning of polymers. *Prog Polym Sci* 2013;38:963–91.
- [23] Doshi J, Srinivasan G, Reneker D. A novel electrospinning process. *Polym News* 1995;20:206–13.
- [24] Ko F, Gogotsi Y, Ali A, Naguib N, Ye H, Yang GL, et al. Electrospinning of continuous carbon nanotube-filled nanofiber yarns. *Adv Mater* 2003;15:1161–5.
- [25] Boghitzki M, Czado W, Frese T, Schaper A, Hellwig M, Steinhart M, et al. Nanostructured fibers via electrospinning. *Adv Mater* 2001;13:70–2.
- [26] Bhardwaj N, Kundu SC. Electrospinning: a fascinating fiber fabrication technique. *Biotechnol Adv* 2010;28:325–47.
- [27] Agarwal S, Greiner A, Wendorff JH. Electrospinning of manmade and biopolymer nanofibers—progress in techniques, materials, and applications. *Adv Funct Mater* 2010;19:2863–79.
- [28] Xie J, Macewan MR, Schwartz AG, Xia Y. Electrospun nanofibers for neural tissue engineering. *Nanoscale* 2010;2:35–44.
- [29] Tian J, Zhao Z, Kumar A, Boughton RI, Liu H. Recent progress in design, synthesis, and applications of one-dimensional TiO<sub>2</sub> nanostructured surface heterostructures: a review. *Chem Soc Rev* 2014;43:6920–37.
- [30] Cavaliere S, Subianto S, Savych I, Jones DJ, Roziere J. Electrospinning: designed architectures for energy conversion and storage devices. *Energy Environ Sci* 2011;4:4761–85.
- [31] Poncelet D, De VP Suter N, Jayasinghe SN. Bio-electrospraying and cell electrospinning: progress and opportunities for basic biology and clinical sciences. *Adv Healthc Mater* 2012;1:27–34.
- [32] Wang M, Jing N, Su CB, Kameoka J, Chou CK, Hung MC, et al. Electrospinning of silica nanochannels for single molecule detection. *Appl Phys Lett* 2006;88, 033106/1–3.
- [33] Kim HW, Song JH, Kim HE. Nanofiber generation of gelatin-hydroxyapatite biomimetics for guided tissue regeneration. *Adv Funct Mater* 2010;15:1988–94.
- [34] Wang X, Ding B, Yu J, Wang M. Engineering biomimetic superhydrophobic surfaces of electrospun nanomaterials. *Nano Today* 2011;6:510–30.
- [35] Li M, Guo Y, Wei Y, Macdiarmid AG, Lelkes PI. Electrospinning polyaniline-contained gelatin nanofibers for tissue engineering applications. *Biomaterials* 2006;27:2705–15.
- [36] Rho KS, Jeong L, Lee G, Seo BM, Park YJ, Hong SD, et al. Electrospinning of collagen nanofibers: effects on the behavior of normal human keratinocytes and early-stage wound healing. *Biomaterials* 2006;27:1452–61.
- [37] Bock N, Dargaville TR, Woodruff MA. Electrospraying of polymers with therapeutic molecules: state of the art. *Prog Polym Sci* 2012;37:1510–51.
- [38] Song J, Klymov A, Shao J, Zhang Y, Ji W, Kolwijk E, et al. Electrospun nanofibrous silk fibroin membranes containing gelatin nanospheres for

- controlled delivery of biomolecules. *Adv Healthc Mater* 2017;6, 1700014/1–10.
- [39] Zhang CL, Yu SH. Nanoparticles meet electrospinning: recent advances and future prospects. *Chem Soc Rev* 2014;43:4423–48.
- [40] Long Y-Z, Yu M, Sun B, Gu C-Z, Fan Z. Recent advances in large-scale assembly of semiconducting inorganic nanowires and nanofibers for electronics, sensors and photovoltaics. *Chem Soc Rev* 2012;41:4560–80.
- [41] Luo CJ, Stoyanov SD, Stride E, Pelan E, Edirisinghe M. Electrospinning versus fibre production methods: from specifics to technological convergence. *Chem Soc Rev* 2012;41:4708–35.
- [42] Sill TJ, Recum HAV. Electrospinning: applications in drug delivery and tissue engineering. *Biomaterials* 2008;29:1989–2006.
- [43] Peng S, Jin G, Li L, Li K, Srinivasan M, Ramakrishna S, et al. Multi-functional electrospun nanofibres for advances in tissue regeneration, energy conversion & storage, and water treatment. *Chem Soc Rev* 2016;45:1225–41.
- [44] Yang DY, Wang Y, Zhang DZ, Liu YY, Jiang XY. Control of the morphology of micro/nanostructures of polycarbonate via electrospinning. *Chin Sci Bull* 2009;54:2911–7.
- [45] Li D, Babel A, Jenekhe SA, Xia Y. Nanofibers of conjugated polymers prepared by electrospinning with a two-capillary spinneret. *Adv Mater* 2004;16:2062–6.
- [46] Li D, Xia YN. Direct fabrication of composite and ceramic hollow nanofibers by electrospinning. *Nano Lett* 2004;4:933–8.
- [47] Loscertales IG, Barrero A, Guerrero I, Cortijo R, Marquez M, Ganan-Calvo AM. Micro/nano encapsulation via electrified coaxial liquid jets. *Science* 2002;295:1695–8.
- [48] Sun Z, Zussman E, Yarin AL, Wendorff JH, Greiner A. Compound core-shell polymer nanofibers by Co-electrospinning. *Adv Mater* 2003;15:1929–32.
- [49] Wang Y, Huang H, Gao J, Lu G, Zhao Y, Xu Y, et al. TiO<sub>2</sub>-SiO<sub>2</sub> composite fibers with tunable interconnected porous hierarchy fabricated by single-spinneret electrospinning toward enhanced photocatalytic activity. *J Mater Chem A Mater Energy Sustain* 2014;2:12442–8.
- [50] Hou Z, Li C, Ma P, Li G, Cheng Z, Peng C, et al. Electrospinning Preparation and Drug-Delivery Properties of an Up-conversion Luminescent Porous NaYF<sub>4</sub>:Yb<sup>3+</sup>, Er<sup>3+</sup>@Silica Fiber Nanocomposite. *Adv Funct Mater* 2011;21:2356–65.
- [51] Zhu Y, Yang DY, Ma HW. One-step fabrication of porous polymeric microgels via electrified jetting. *Nanoscale* 2010;2:910–2.
- [52] Pai CL, Boyce MC, Rutledge GC. Morphology of porous and wrinkled fibers of polystyrene electrospun from Dimethylformamide. *Macromolecules* 2009;42:2102–14.
- [53] McCann JT, Marquez M, Xia YN. Highly porous fibers by electrospinning into a cryogenic liquid. *J Am Chem Soc* 2006;128:1436–7.
- [54] Fong H, Chun I, Reneker DH. Beaded nanofibers formed during electrospinning. *Polymer* 1999;40:4585–92.
- [55] Chen H, And JDS, Elabd YA. Electrospinning and solution properties of nafion and poly(acrylic acid). *Macromolecules* 2008;41:128–35.
- [56] Duan B, Yuan X, Zhu Y, Zhang Y, Li X, Zhang Y, et al. A nanofibrous composite membrane of PLGA-chitosan/PVA prepared by electrospinning. *Eur Polym J* 2006;42:2013–22.
- [57] Wu L, Yuan X, Sheng J. Immobilization of cellulase in nanofibrous PVA membranes by electrospinning. *J Membr Sci* 2005;250:167–73.
- [58] Duan B, Dong CH, Yuan XY, Yao KD. Electrospinning of chitosan solutions in acetic acid with poly(ethylene oxide). *J Biomat Sci Polym Ed* 2004;15:797–811.
- [59] Zhang C, Yuan X, Wu L, Han Y, Sheng J. Study on morphology of electrospun poly(vinyl alcohol) mats. *Eur Polym J* 2005;41:423–32.
- [60] Zussman E, Yarin AL, Bazilevsky AV, Avrahami R, Feldman M. Electrospun Polyaniiline/Poly(methyl methacrylate)-Derived Turbostratic Carbon Micro-/Nanotubes. *Adv Mater* 2006;18:348–53.
- [61] Dror Y, Salalha W, Avrahami R, Zussman E, Yarin AL, Dersch R, et al. One-step production of polymeric microtubes by co-electrospinning. *Small* 2007;3:1064–73.
- [62] Ji X, Wang P, Su Z, Ma G, Zhang S. Enabling multi-enzyme biocatalysis using coaxial-electrospun hollow nanofibers: redesign of artificial cells. *J Mater Chem B Mater Biol Med* 2013;2:181–90.
- [63] He G, Cai Y, Zhao Y, Wang X, Lai C, Xi M, et al. Electrospun anatase-phase TiO<sub>2</sub> nanofibers with different morphological structures and specific surface areas. *J Colloid Interface Sci* 2013;398:103–11.
- [64] Chen H, Wang N, Di J, Zhao Y, Song Y, Jiang L. Nanowire-in-microtube structured core/shell fibers via multifluidic coaxial electrospinning. *Langmuir* 2010;26:11291–6.
- [65] Zhao Y, Cao X, Jiang L. Bio-mimic multichannel microtubes by a facile method. *J Am Chem Soc* 2007;129:764–5.
- [66] Si Y, Wang L, Wang X, Tang N, Yu J, Ding B. Ultrahigh-Water-Content, Superelastic, and Shape-Memory Nanofiber-Assembled Hydrogels Exhibiting Pressure-Responsive Conductivity. *Adv Mater* 2017;29, 1700339/1–7.
- [67] Liu J, Jiang G, Liu Y, Di J, Wang Y, Zhao Z, et al. Hierarchical macro-meso-microporous ZSM-5 zeolite hollow fibers with highly efficient catalytic cracking capability. *Sci Rep* 2014;4, 7276/1–6.
- [68] Lee BS, Jeon SY, Park H, Lee G, Yang HS, Yu WR. New electrospinning nozzle to reduce jet instability and its application to manufacture of multi-layered nanofibers. *Sci Rep* 2014;4, 6758/1–9.
- [69] Wang N, Chen H, Lin L, Zhao Y, Cao X, Song Y, et al. Multicomponent phase change microfibers prepared by temperature control multifluidic electrospinning. *Macromol Rapid Commun* 2010;31:1622–7.
- [70] Cooper AI. Porous materials and supercritical fluids. *Adv Mater* 2003;15:1049–59.
- [71] Davis ME. Ordered porous materials for emerging applications. *Nature* 2002;417:813–21.
- [72] Bognitzki M, Frese T, Steinhart M, Greiner A, Wendorff JH, Schaper A, et al. Preparation of fibers with nanoscaled morphologies: electrospinning of polymer blends. *Polym Eng Sci* 2001;41:982–9.
- [73] Zhang YZ, Feng Y, Huang ZM, Ramakrishna S, Lim CT. Fabrication of porous electrospun nanofibres. *Nanotechnology* 2006;17:901–8.
- [74] You Y, Ji HY, Lee SW, Min BM, Lee SJ, Park WH. Preparation of porous ultrafine PGA fibers via selective dissolution of electrospun PGA / PLA blend fibers. *Mater Lett* 2006;60:757–60.
- [75] Lin JY, Ding B, Yu JY, Hsieh Y. Direct fabrication of highly nanoporous polystyrene fibers via electrospinning. *ACS Appl Mater Interfaces* 2010;2:521–8.
- [76] Dayal P, Liu J, Kumar S, Kyu Thein. Experimental and theoretical investigations of porous structure formation in electrospun fibers. *Macromolecules* 2007;40:7689–94.
- [77] Yano T, Weng OY, Yamaguchi H, Terayama Y, Nishihara M, Kobayashi M, et al. Precise control of surface physicochemical properties for electrospun fiber mats by surface-initiated radical polymerization. *Polym J* 2011;43:838–48.
- [78] Sun D, Qin G, Miao L, Wei W, Wang N, Jiang L. Preparation of mesoporous polyacrylonitrile and carbon fibers by electrospinning and supercritical drying. *Carbon* 2013;63:585–8.
- [79] Yazgan G, Dmitriev RI, Tyagi V, Jenkins J, Rotaru G-M, Rottmar M, et al. Steering surface topographies of electrospun fibers: understanding the mechanisms. *Sci Rep* 2017;7, 158/1–13.
- [80] Megelski S, Stephens JS, Chase DB, Rabolt JF. Micro- and nanostructured surface morphology on electrospun polymer fibers. *Macromolecules* 2002;35:8456–66.
- [81] Wang N, Gao Y, Wang YX, Liu K, Lai W, Hu Y, et al. Nanoengineering to achieve high sodium storage: a case study of carbon coated hierarchical nanoporous TiO<sub>2</sub> microfibers. *Adv Sci* 2016;3, 1600013/1–7.
- [82] Li D, McCann JT, Gratt M, Xia Y. Photocatalytic deposition of gold nanoparticles on electrospun nanofibers of titania. *Chem Phys Lett* 2004;394:387–91.
- [83] Formica FA, Ozturk E, Hess SC, Stark WJ, Maniura-Weber K, Rottmar M, et al. A bioinspired ultraporous nanofiber-hydrogel mimic of the cartilage extracellular matrix. *Adv Healthc Mater* 2016;5:3129–38.
- [84] Yu Y, Gu L, Zhu C, Aken PAV, Maier J. Tin nanoparticles encapsulated in porous multichannel carbon microtubes: preparation by single-nozzle electrospinning and application as anode material for high-performance Li-Based batteries. *J Am Chem Soc* 2009;131:15984–5.
- [85] Hansen NS, Cho D, Joo YL. Metal nanofibers with highly tunable electrical and magnetic properties via highly loaded water-based electrospinning. *Small* 2012;8:1510–4.
- [86] Zhu Y, Han X, Yu Y, Liu Y, Zheng S, Xu K, et al. Electrospun Sb/C fibers for a stable and fast sodium-ion battery anode. *ACS Nano* 2013;7:6378–86.
- [87] Tian W, Zhai TY, Zhang C, Li SL, Wang X, Liu F, et al. Low-cost fully transparent ultraviolet photodetectors based on electrospun ZnO-SnO<sub>2</sub> heterojunction nanofibers. *Adv Mater* 2013;25:4625–30.
- [88] Ostermann R, Li D, Yin Y, McCann JT, Xia Y. V<sub>2</sub>O<sub>5</sub> nanorods on TiO<sub>2</sub> nanofibers: a new class of hierarchical nanostructures enabled by electrospinning and calcination. *Nano Lett* 2006;6:1297–302.
- [89] Lin DD, Wu H, Pan W. Photoswitches and memories assembled by electrospinning aluminum-doped zinc oxide single nanowires. *Adv Mater* 2007;19:3968–72.
- [90] Zhang F, Yuan C, Zhu J, Wang J, Zhang X, Lou XW. Capacitors: Flexible Films Derived from Electrospun Carbon Nanofibers Incorporated with Co<sub>3</sub>O<sub>4</sub> Hollow Nanoparticles as Self-Supported Electrodes for Electrochemical Capacitors. *Adv Funct Mater* 2013;23:3909–15.
- [91] Zhu C, Yu Y, Gu L, Weichert K, Maier J. Electrospinning of highly electroactive carbon-coated single-crystalline LiFePO<sub>4</sub> nanowires. *Angew Chem Int Ed* 2011;50:6278–82.
- [92] Yao H, Zheng G, Hsu PC, Kong D, Cha JJ, Li W, et al. Improving lithium-sulphur batteries through spatial control of sulphur species deposition on a hybrid electrode surface. *Nat Commun* 2014;5:3943–51.
- [93] Lee BL, Jeon H, Wang A, Yan Z, Yu J, Grigoropoulos C, et al. Femtosecond laser ablation enhances cell infiltration into three-dimensional electrospun scaffolds. *Acta Biomater* 2012;8:2648–58.
- [94] Cho JS, Lee SY, Kang YC. First Introduction of NiSe<sub>2</sub>to Anode Material for Sodium-Ion Batteries: A Hybrid of Graphene-Wrapped NiSe<sub>2</sub>/C Porous Nanofiber. *Sci Rep* 2016;6, 23338/1–10.
- [95] Lu X, Zhao Y, Wang C. Fabrication of PbS nanoparticles in polymer-fiber matrices by electrospinning. *Adv Mater* 2005;17:2485–8.
- [96] Bai J, Li Y, Yang S, Du J, Wang S, Zhang C, et al. Synthesis of AgCl/PAN composite nanofibres using an electrospinning method. *Nanotechnology* 2007;18:410–5.
- [97] Bognitzki M, Becker M, Graeser M, Massa W, Wendorff JH, Schaper A, et al. Preparation of sub-micrometer copper fibers via electrospinning. *Adv Mater* 2006;18:2384–6.

- [98] Wu H, Hu L, Rowell MW, Kong D, Cha JJ, McDonough JR, et al. Electrospun metal nanofiber webs as high-performance transparent electrode. *Nano Lett* 2010;10:4242–8.
- [99] Ghafoor S, Ata S, Mahmood N, Arshad SN. Photosensitization of TiO<sub>2</sub> nanofibers by Ag2S with the synergistic effect of excess surface Ti(3+) states for enhanced photocatalytic activity under simulated sunlight. *Sci Rep* 2017;7, 255/1–10.
- [100] Solarajan AK, Murugadoss V, Angaiah S. Dimensional stability and electrochemical behaviour of ZrO<sub>2</sub> incorporated electrospun PVdF-HFP based nanocomposite polymer membrane electrolyte for Li-ion capacitors. *Sci Rep* 2017;7, 45390/1–9.
- [101] Kim M, Kwon C, Eom K, Kim J, Cho E. Electrospun Nb-doped TiO<sub>2</sub> nanofiber support for Pt nanoparticles with high electrocatalytic activity and durability. *Sci Rep* 2017;7, 44411/1–8.
- [102] Meng X, Shin DW, Yu SM, Jung JH, Hong IK, Lee HM, Han YH, et al. Growth of hierarchical TiO<sub>2</sub> nanostructures on anatase nanofibers and their application in photocatalytic activity. *CrystEngComm* 2011;13:3021–9.
- [103] Jin Y, Yang D, Kang D, Jiang X. Fabrication of necklace-like structures via electrospinning. *Langmuir* 2010;26:1186–90.
- [104] Liu X, Gu L, Zhang Q, Wu J, Long Y, Fan Z. All-printable band-edge modulated ZnO nanowire photodetectors with ultra-high detectivity. *Nat Commun* 2014;5:4007–15.
- [105] Niu C, Meng J, Wang X, Han C, Yan M, Zhao K, et al. General synthesis of complex nanotubes by gradient electrospinning and controlled pyrolysis. *Nat Commun* 2015;6:7402–10.
- [106] Zhang Y, Shuai Y, Xiao F, Li H, Zhou J, Bo W. Preparation of nanofibrous metal-organic framework filters for efficient air pollution control. *J Am Chem Soc* 2016;138:5785–8.
- [107] Hsu CY, Liu YL. Rhodamine B-anchored silica nanoparticles displaying white-light photoluminescence and their uses in preparations of photoluminescent polymeric films and nanofibers. *J Colloid Interface Sci* 2010;350:75–82.
- [108] Shi W, Song S, Zhang H. Hydrothermal synthetic strategies of inorganic semiconducting nanostructures. *Chem Soc Rev* 2013;42:5714–43.
- [109] Reysenbach AL, Shock E. Merging genomes with geochemistry in hydrothermal ecosystems. *Science* 2002;296:1077–82.
- [110] Feng S, Xu R. New materials in hydrothermal synthesis. *Acc Chem Res* 2001;34:239–47.
- [111] Chen Y, Lu Z, Zhou L, Mai YW, Huang H. Triple-coaxial electrospun amorphous carbon nanotubes with hollow graphitic carbon nanospheres for high-performance Li ion batteries. *Energy Environ Sci* 2012;5:7898–902.
- [112] Hsu PC, Wu H, Carney TJ, McDowell MT, Yang Y, Garnett EC, et al. Passivation coating on electrospun copper nanofibers for stable transparent electrodes. *ACS Nano* 2012;6:5150–6.
- [113] Hsu PC, Wang S, Wu H, Narasimhan VK, Kong D, Ryoung LH, et al. Performance enhancement of metal nanowire transparent conducting electrodes by mesoscale metal wires. *Nat Commun* 2013;4:2522–8.
- [114] Chen R, Zhao S, Han G, Dong J. Fabrication of the silver/polypyrrole/polyacrylonitrile composite nanofibrous mats. *Mater Lett* 2008;62:4031–4.
- [115] Xiao S, Ma H, Shen M, Wang S, Huang Q, Shi X. Excellent copper(II) removal using zero-valent iron nanoparticle-immobilized hybrid electrospun polymer nanofibrous mats. *Colloids Surf A Physicochem Eng Asp* 2011;381:48–54.
- [116] Shi Q, Vitchuli N, Nowak J, Noar J, Caldwell JM, Breidt F, et al. One-step synthesis of silver nanoparticle-filled nylon 6 nanofibers and their antibacterial properties. *J Mater Chem* 2011;21:10330–5.
- [117] Yang DJ, Kamiencik I, Youn DY, Rothschild A, Kim ID. Ultrasensitive and highly selective gas sensors based on electrospun SnO<sub>2</sub> nanofibers modified by Pd loading. *Adv Funct Mater* 2010;20:4258–64.
- [118] Dong H, Fey E, Gandelman A, Jones Jr WE. Synthesis and assembly of metal nanoparticles on electrospun poly(4-vinylpyridine) fibers and poly(4-vinylpyridine) composite fibers. *Chem Mater* 2006;18:2008–11.
- [119] Ji SC, Kim HS, Yoo HS. Electrospinning strategies of drug-incorporated nanofibrous mats for wound recovery. *Drug Deliv Transl Res* 2015;5:137–45.
- [120] Hou Z, Li X, Li C, Dai Y, Ma P, Zhang X, et al. Electrospun upconversion composite fibers as dual drugs delivery system with individual release properties. *Langmuir* 2013;29:9473–82.
- [121] Xu X, Chen X, Ma P, Wang X, Jing X. The release behavior of doxorubicin hydrochloride from medicated fibers prepared by emulsion-electrospinning. *Eur J Pharm Biopharm* 2008;70:165–70.
- [122] Qin XH, Wu DQ, Chu CC. Dual functions of polyvinyl alcohol (PVA): fabricating particles and electrospinning nanofibers applied in controlled drug release. *J Nanopart Res* 2013;15, 1395/1–14.
- [123] Naveen N, Kumar R, Balaji S, Uma TS, Natrajan TS, Sehgal PK. Synthesis of nonwoven nanofibers by electrospinning - a promising biomaterial for tissue engineering and drug delivery. *Adv Eng Mater* 2010;12:B380–7.
- [124] Liao I, Chen S, Liu J, Leong K. Sustained viral gene delivery through core-shell fibers. *J Control Release* 2009;139:48–55.
- [125] Yau WW, Long H, Gauthier NC, Chan JK, Chew SY. The effects of nanofiber diameter and orientation on siRNA uptake and gene silencing. *Biomaterials* 2015;37:94–106.
- [126] Fang Z, Jia X, Yang Y, Yang Q, Chao G, Zhao Y, et al. Peptide-modified PEI/CL electrospun membranes for regulation of vascular endothelial cells. *Mat Sci Eng C* 2016;68:623–31.
- [127] Zhou F, Jia X, Yang Y, Yang Q, Gao C, Hu S, et al. Nanofiber-mediated microRNA-126 delivery to vascular endothelial cells for blood vessel regeneration. *Acta Biomater* 2016;43:303–13.
- [128] Xia H, Jun J, Wenping L, Yifeng P, Xiaoling C. Chitosan nanoparticle carrying small interfering RNA to platelet-derived growth factor B mRNA inhibits proliferation of smooth muscle cells in rabbit injured arteries. *Vascular* 2013;21:301–6.
- [129] Chen M, Gao S, Dong M, Song J, Yang C, Howard KA, et al. Chitosan/siRNA nanoparticles encapsulated in PLGA nanofibers for siRNA delivery. *ACS Nano* 2012;6:4835–44.
- [130] Katas H, Alpar HO. Development and characterisation of chitosan nanoparticles for siRNA delivery. *J Control Release* 2006;115:216–25.
- [131] Lai HJ, Kuan CH, Wu HC, Tsai JC, Chen TM, Hsieh DJ, et al. Tailor design electrospun composite nanofibers with staged release of multiple angiogenic growth factors for chronic wound healing. *Acta Biomater* 2014;10:4156–66.
- [132] Kadirkelvuru K, Fathima NN. Self-assembly of keratin peptides: its implication on the performance of electrospun PVA nanofibers. *Sci Rep* 2016;6, 36558/1–9.
- [133] Cao H, Jiang X, Chai C, Chew SY. RNA interference by nanofiber-based siRNA delivery system. *J Control Release* 2010;144:203–12.
- [134] Luu YK, Kim K, Hsiao BS, Chu B, Hadjargyrou M. Development of a nanostructured DNA delivery scaffold via electrospinning of PLGA and PLA-PEG block copolymers. *J Control Release* 2003;89:341–53.
- [135] Saraf A, Baggett LS, Raphael RM, Kasper FK, Mikos AG. Regulated non-viral gene delivery from coaxial electrospun fiber mesh scaffolds. *J Control Release* 2010;143:95–103.
- [136] Salvay DM, Zelyvianskaya M, Shea LD. Gene delivery by surface immobilization of plasmid to tissue-engineering scaffolds. *Gene Ther* 2010;17:1134–41.
- [137] Liu Y, Lu J, Li H, Wei J, Li X. Engineering blood vessels through micropatterned co-culture of vascular endothelial and smooth muscle cells on bilayered electrospun fibrous mats with pDNA inoculation. *Acta Biomater* 2015;11:114–25.
- [138] Nguyen LH, Gao M, Lin J, Wu W, Wang J, Chew SY. Three-dimensional aligned nanofibers-hydrogel scaffold for controlled non-viral drug/gene delivery to direct axon regeneration in spinal cord injury treatment. *Sci Rep* 2017;7, 42212/1–12.
- [139] James EN, Delany AM, Nair LS. Post-transcriptional regulation in osteoblasts using localized delivery of miR-29a inhibitor from nanofibers to enhance extracellular matrix deposition. *Acta Biomater* 2014;10:3571–80.
- [140] And SWL, Belcher AM. Virus-based fabrication of Micro- and nanofibers using electrospinning. *Nano Lett* 2004;4:387–90.
- [141] Gensheimer M, Becker M, Brandis-Heep A, Wendorff JH, Thauer RK, Greiner A. Novel biohybrid materials by electrospinning: nanofibers of poly(ethylene oxide) and living bacteria. *Adv Mater* 2007;19:2480–2.
- [142] Liu Y, Rafailovich MH, Malal R, Cohn D, Chidambaram D, Demain AL. Engineering of bio-hybrid materials by electrospinning polymer-microbe fibers. *Proc Natl Acad Sci USA* 2009;106:14201–6.
- [143] Han J, Liang C, Cui Y, Xiong L, Guo X, Yuan X, et al. Encapsulating microorganisms inside electrospun microfibers as a living material enables room-temperature storage of microorganisms. *ACS Appl Mater Interfaces* 2018;10:38799–806.
- [144] Zussman E. Encapsulation of cells within electrospun fibers. *Polym Adv Technol* 2011;22:366–71.
- [145] Klein S, Kuhn J, Avrahami R, Tarre S, Beliavski M, Green M, et al. Encapsulation of bacterial cells in Electrospun Microtubes. *Biomacromolecules* 2009;10:1751–6.
- [146] Charles KJ, Eyal Z. Encapsulation of bacteria and viruses in electrospun fibers. *Nanotechnology* 2006;17:4675–81.
- [147] Letnik I, Avrahami R, Rokem JS, Greiner A, Zussman E, Greenblatt C. Living composites of electrospun yeast cells for bioremediation and ethanol production. *Biomacromolecules* 2015;16:3322–8.
- [148] Gensheimer M, Brandisheep A, Agarwal S, Thauer RK, Greiner A. Polymer/bacteria composite nanofiber non-wovens by electrospinning of living bacteria protected by hydrogel microparticles. *Macromol Biosci* 2011;11:333–7.
- [149] Townsend-Nicholson A, Jayasinghe SN. Cell electrospinning: a unique biotechnique for encapsulating living organisms for generating active biological microthreads/scaffolds. *Biomacromolecules* 2006;7:3364–9.
- [150] Shi Q, Hou J, Zhao C, Xin Z, Jin J, Li C, et al. A smart core-sheath nanofiber that captures and releases red blood cells from the blood. *Nanoscale* 2016;8:2022–9.
- [151] Lin T, Wang H, Wang X. Self-crimping bicomponent nanofibers electrospun from Polyacrylonitrile and elastomeric polyurethane. *Adv Mater* 2005;17:2699–703.
- [152] Kota AK, Kwon G, Tuteja A. The design and applications of superomniphobic surfaces. *NPG Asia Mater* 2014;6:109–24.
- [153] Bin D, Lili W, Xiaoran L, Xiaoyan Y, Xiulan L, Yang Z, et al. Degradation of electrospun PLGA-chitosan/PVA membranes and their cytocompatibility in vitro. *J Biomater Sci Polym Ed* 2007;18:95–115.
- [154] Xu CY, Inai R, Kotaki M, Ramakrishna S. Aligned biodegradable nanofibrous structure: a potential scaffold for blood vessel engineering. *Biomaterials* 2004;25:877–86.

- [155] Bhattacharai SR, Bhattacharai N, Yi HK, Hwang PH, Cha DI, Kim HY. Novel biodegradable electrospun membrane: scaffold for tissue engineering. *Biomaterials* 2004;25:2595–602.
- [156] Arras MML, Jana R, Mühlstädt M, Maenz S, Andrews J, Su Z, et al. In situ formation of nanohybrid shish-kebabs during electrospinning for the creation of hierarchical shish-kebab structures. *Macromolecules* 2016;49:3550–8.
- [157] Yin Z, Chen X, Chen JL, Shen WL, Hieu Nguyen TM, Gao L, et al. The regulation of tendon stem cell differentiation by the alignment of nanofibers. *Biomaterials* 2010;31:2163–75.
- [158] Xu H, Cui W, Chang J. Fabrication of patterned PDLLA/PCL composite scaffold by electrospinning. *J Appl Polym Sci* 2012;127:1550–4.
- [159] Li D, Wang Y, Xia Y. Electrospinning of polymeric and ceramic nanofibers as uniaxially aligned arrays. *Nano Lett* 2003;3:1167–71.
- [160] Li D, Ouyang G, Mccann JT, Xia Y. Collecting electrospun nanofibers with patterned electrodes. *Nano Lett* 2005;5:913–6.
- [161] Xiao Y, Zhang B, Liu H, Miklas JW, Gagliardi M, Pahnke A, et al. Microfabricated perfusible cardiac biowire: a platform that mimics native cardiac bundle. *Lab Chip* 2014;14:869–82.
- [162] Zhe L, Liu C, Li L, Xu P, Luo G, Ding M, et al. Double-network hydrogel with tunable mechanical performance and biocompatibility for the fabrication of stem cells-encapsulated fibers and 3D assemble. *Sci Rep* 2016;6:33462/1–11.
- [163] He J, Zhou Y, Qi K, Wang L, Li P, Cui S. Continuous twisted nanofiber yarns fabricated by double conjugate electrospinning. *Fiber Polym* 2013;14:1857–63.
- [164] Okuzaki H, Takahashi T, Miyajima N, Suzuki Y, Kuwabara T. Spontaneous formation of poly(p-phenylenevinylene) nanofiber yarns through electrospinning of a precursor. *Macromolecules* 2006;39:4276–8.
- [165] Wang X, Zhang K, Zhu M, Yu H, Zhou Z, Chen Y, et al. Continuous polymer nanofiber yarns prepared by self-bundling electrospinning method. *Polymer* 2008;49:2755–61.
- [166] Teo WE, Gopal R, Ramaseshan R, Fujihara K, Ramakrishna S. A dynamic liquid support system for continuous electrospun yarn fabrication. *Polymer* 2007;48:3400–5.
- [167] Smit E, Büttner U, Sanderson RD. Continuous yarns from electrospun fibers. *Polymer* 2005;46:2419–23.
- [168] Pan H, Li L, Hu L, Cui X. Continuous aligned polymer fibers produced by a modified electrospinning method. *Polymer* 2006;47:4901–4.
- [169] Yuan H, Zhao S, Tu H, Li B, Li Q, Feng B, et al. Stable jet electrospinning for easy fabrication of aligned ultrafine fibers. *J Mater Chem* 2012;22:19634–8.
- [170] Shin YM, Hohman MM, Brenner MP, Rutledge GC. Electrospinning: a whipping fluid jet generates submicron polymer fibers. *Appl Phys Lett* 2001;78:1149–51.
- [171] Ding W, Wei S, Zhu J, Chen X, Dan R, Guo Z. Manipulated electrospun PVA nanofibers with inexpensive salts. *Macromol Mater Eng* 2010;295:958–65.
- [172] Qin X, Wu D. Effect of different solvents on poly(caprolactone) (PCL) electrospun nonwoven membranes. *J Therm Anal Calorim* 2012;107:1007–13.
- [173] Li M, Yang D, Long Y, Ma H. Arranging junctions for nanofibers. *Nanoscale* 2010;2:218–21.
- [174] Liguori A, Bigi A, Colombo V, Focarete ML, Gherardi M, Gualandi C, et al. Atmospheric Pressure Non-Equilibrium Plasma as a Green Tool to Crosslink Gelatin Nanofibers. *Sci Rep* 2016;6:38542/1–11.
- [175] Si Y, Yu J, Tang X, Ge J, Ding B. Ultralight nanofibre-assembled cellular aerogels with superelasticity and multifunctionality. *Nat Commun* 2014;5:5802–10.
- [176] Matthews JA, Wnek GE, Simpson DG, Bowlin GL. Electrospinning of collagen nanofibers. *Biomacromolecules* 2002;3:232–8.
- [177] Yang D, Lu B, Zhao Y, Jiang X. Fabrication of aligned fibrous arrays by magnetic electrospinning. *Adv Mater* 2007;19:3702–6.
- [178] Li M, Long YZ, Yang D, Sun J, Yin H, Zhao Z, et al. Fabrication of one dimensional superfine polymer fibers by double-spinning. *J Mater Chem* 2011;21:13159–62.
- [179] Katta P, Alessandro M, And RDR, Chase GG. Continuous electrospinning of aligned polymer nanofibers onto a wire drum collector. *Nano Lett* 2004;4:2215–8.
- [180] Corey JN, Lin DY, Mycek KB, Chen Q, Samuel S, Feldman EL, et al. Aligned electrospun nanofibers specify the direction of dorsal root ganglia neurite growth. *J Biomed Mater Res A* 2007;83:636–45.
- [181] Huang ZM, Zhang YZ, Kotaki M, Ramakrishna S. A review on polymer nanofibers by electrospinning and their applications in nanocomposites. *Compos Sci Technol* 2003;63:2223–53.
- [182] Sundaray B, Subramanian V, Natarajan TS, Xiang RZ, Chang CC, Fann WS. Electrospinning of continuous aligned polymer fibers. *Appl Phys Lett* 2004;84:1222–4.
- [183] Zussman E, Theron A, Yarin AL. Formation of nanofiber crossbars in electrospinning. *Appl Phys Lett* 2003;82:973–5.
- [184] Theron A, Zussman E, Yarin AL. Electrostatic field-assisted alignment of electrospun nanofibres. *Nanotechnology* 2001;12:384–90.
- [185] Li D, Wang Y, Xia Y. Electrospinning nanofibers as uniaxially aligned arrays and layer-by-Layer stacked films. *Adv Mater* 2004;16:361–6.
- [186] Dabirian F, Sarkeshik S, Kianiha A. Production of uniaxially aligned nanofibers using a modified electrospinning method: rotating jet. *Curr Nanosci* 2009;5:318–23.
- [187] Khamforoush M, Mahjob M. Modification of the rotating jet method to generate highly aligned electrospun nanofibers. *Mater Lett* 2011;65:453–5.
- [188] Taskin MB, Xu R, GregerSEN H, Nygaard JV, Besenbacher F, Chen M. Three-dimensional polydopamine functionalized coiled microfibrous scaffolds enhance human mesenchymal stem cells colonization and mild myofibroblastic differentiation. *ACS Appl Mater Interfaces* 2016;8:15864–73.
- [189] Veretennikov I, Indeikina A, Chang HC, Marquez M, Suib SL, Giraldo O. Mechanism for helical gel formation from evaporation of colloidal solutions. *Langmuir* 2002;18:8792–8.
- [190] Giraldo O, Brock SL, Marquez M, Suib SL, Hillhouse H, Tsapatsis M. Spontaneous formation of inorganic helices. *Nature* 2000;405:38.
- [191] Kessick R, Tepper G. Microscale polymeric helical structures produced by electrospinning. *Appl Phys Lett* 2004;84:4807–9.
- [192] Chen S, Hou H, Hu P, Wendorff JH, Greiner A, Agarwal S. Polymeric nanosprings by bicomponent electrospinning. *Macromol Mater Eng* 2010;294:265–71.
- [193] Silva PES, Godinio MH. Helical microfilaments with alternating imprinted intrinsic curvatures. *Macromol Rapid Commun* 2017;38, 1600700/1–8.
- [194] Ansorge HL, Adams S, Birk DE. Mechanical, compositional, and structural properties of the post-natal mouse achilles tendon. *Ann Biomed Eng* 2011;39:1904–13.
- [195] Zhang G, Young BB, Ezura Y, Favata M, Soslowsky LJ, Chakravarti S, et al. Development of tendon structure and function: regulation of collagen fibrillogenesis. *J Musculoskelet Neuron Interact* 2005;5:5–21.
- [196] Franchi M, Fini M, Quaranta M, Pasquale VD, Raspanti M, Giavaresi G, et al. Crimp morphology in relaxed and stretched rat Achilles tendon. *J Anat* 2007;210:1–7.
- [197] Liu W, Lipner J, Moran CH, Feng L, Li X, Thomopoulos S, et al. Generation of electrospun nanofibers with controllable degrees of crimping through a simple, plasticizer-based treatment. *Adv Mater* 2015;27:2583–8.
- [198] Park S, Son CW, Lee S, Kim DY, Park C, Eom KS, et al. Multicore-shell nanofiber architecture of polyimide/polyvinylidene fluoride blend for thermal and long-term stability of lithium ion battery separator. *Sci Rep* 2016;6, 36977/1–8.
- [199] Zhang D, Chang J. Electrospinning of three-dimensional nanofibrous tubes with controllable architectures. *Nano Lett* 2008;8:3283–7.
- [200] Tao H, Li Q, Hua D, Xiao W, Ling L, Cao X. Patterning electrospun nanofibers via agarose hydrogel stamps to spatially coordinate cell orientation in microfluidic device. *Small* 2017;13, 1602610/1–7.
- [201] Sun Daoheng, Chang Chieh, Li S, Lin Liwei. Near-field electrospinning. *Nano Lett* 2006;6:839–42.
- [202] Hochleitner G, Hümmel JF, Luxenhofer R, Groll J. High definition fibrous poly(2-ethyl-2-oxazoline) scaffolds through melt electrospinning writing. *Polymer* 2014;55:5017–23.
- [203] Jeong YH, Lee J. Fabrication of microfiber patterns with ivy shoot-like geometries using improved electrospinning. *Materials* 2016;9:266–76.
- [204] Rogers CM, Morris GE, Gould TW, Bail R, Toumpaniari S, Harrington H, et al. A novel technique for the production of electrospun scaffolds with tailored three-dimensional micro-patterns employing additive manufacturing. *Biofabrication* 2014;6, 035003/1–11.
- [205] McClure MJ, Wolfe PS, Simpson DG, Sell SA, Bowlin GL. The use of air-flow impedance to control fiber deposition patterns during electrospinning. *Biomaterials* 2012;33:771–9.
- [206] Jia C, Yu D, Lamarre M, Leopold PL, Teng YD, Wang H. Patterned electrospun nanofiber matrices via localized dissolution: potential for guided tissue formation. *Adv Mater* 2014;26:8192–7.
- [207] Brown TD, Edin F, Dettla N, Skelton AD, Hutmacher DW, Dalton PD. Melt electrospinning of poly( $\epsilon$ -caprolactone) scaffolds: phenomenological observations associated with collection and direct writing. *Mat Sci Eng C* 2015;45:698–708.
- [208] Zhang D, Chang J. Patterning of electrospun fibers using electroconductive templates. *Adv Mater* 2007;19:3664–7.
- [209] Brown TD, Dalton PD, Hutmacher DW. Direct writing by way of melt electrospinning. *Adv Mater* 2011;23:5651–7.
- [210] Kakunuri M, Wanasekara ND, Sharma CS, Khandelwal M, Eichhorn SJ. Three-dimensional electrospun micropatterned cellulose acetate nanofiber surfaces with tunable wettability. *J Appl Polym Sci* 2017;134, 44709/1–7.
- [211] Visser J, Melchels FP, Jeon JE, van Bussel EM, Kimpton LS, Byrne HM, et al. Reinforcement of hydrogels using three-dimensionally printed microfibres. *Nat Commun* 2015;6:6933–42.
- [212] Park SM, Kim DS. Electrospinning: electrolyte-assisted electrospinning for a self-assembled, free-standing nanofiber membrane on a curved surface. *Adv Mater* 2015;27:1682–7.
- [213] Jo HS, An S, Lee J-G, Park HG, Al-Deyab SS, Yarin AL, et al. Highly flexible, stretchable, patternable, transparent copper fiber heater on a complex 3D surface. *NPG Asia Mater* 2017;9, e347/1–7.
- [214] Sun B, Long YZ, Zhang HD, Li MM, Duvail JL, Jiang XY, et al. Advances in three-dimensional nanofibrous macrostructures via electrospinning. *Prog Polym Sci* 2014;39:862–90.
- [215] Andersson RL, Ström V, Gedde UW, Mallon PE, Hedenqvist MS, Olsson RT. Micromechanics of ultra-toughened electrospun PMMA/PEO fibres as revealed by in-situ tensile testing in an electron microscope. *Sci Rep* 2014;4, 6335/1–8.
- [216] Dalton PD, Klee D, Möller M. Electrospinning with dual collection rings. *Polymer* 2005;46:611–4.

- [217] Liu LQ, Eder M, Burgert I, Tasis D, Prato M, Wagner HD. One-step electrospun nanofiber-based composite ropes. *Appl Phys Lett* 2007;90: 083108/1–3.
- [218] Cheng H, Hu C, Zhao Y, Qu L. Graphene fiber: a new material platform for unique applications. *NPG Asia Mater* 2014;6: e113/1–13.
- [219] Deravi LF, Sinatra NR, Chantre CO, Nesmith AP, Yuan H, Deravi SK, et al. Design and fabrication of fibrous nanomaterials using pull spinning. *Macromol Mater Eng* 2017;302: 1600404/1–14.
- [220] Yuan B, Jin Y, Sun Y, Wang D, Sun J, Wang Z, et al. A strategy for depositing different types of cells in three dimensions to mimic tubular structures in tissues. *Adv Mater* 2012;24:890–6.
- [221] Seliktar D, Nerem RM, Galis ZS. The role of matrix metalloproteinase-2 in the remodeling of cell-seeded vascular constructs subjected to cyclic strain. *Ann Biomed Eng* 2001;29:923–34.
- [222] Lam MT, Huang YC, Birla RK, Takayama S. Microfeature guided skeletal muscle tissue engineering for highly organized 3-dimensional free-standing constructs. *Biomaterials* 2009;30:1150–5.
- [223] Yousefzadeh M, Latifi M, Amani-Tehran M, Teo WE, Ramakrishna S. A note on the 3D structural design of electrospun nanofibers. *J Eng Fiber Fabr* 2012;7:17–23.
- [224] Brewster LP, Bufallino D, Ucuzian A, Greisler HP. Growing A living Blood Vessel: insights for the second hundred years. *Biomaterials* 2007;28:5028–32.
- [225] Zhang H, Jia X, Han F, Zhao J, Zhao Y, Fan Y, et al. Dual-delivery of VEGF and PDGF by double-layered electrospun membranes for blood vessel regeneration. *Biomaterials* 2013;34:2202–12.
- [226] Han F, Jia X, Dai D, Yang X, Zhao J, Zhao Y, et al. Performance of a multilayered small-diameter vascular scaffold dual-loaded with VEGF and PDGF. *Biomaterials* 2013;34:7302–13.
- [227] Gong P, Zheng W, Huang Z, Zhang W, Xiao D, Jiang X. A strategy for the construction of controlled, three-dimensional, multilayered, tissue-like structures. *Adv Funct Mater* 2013;23:42–6.
- [228] Mo XM, Xu CY, Kotaki M, Ramakrishna S. Electrospun P(LLA-CL) nanofiber: a biomimetic extracellular matrix for smooth muscle cell and endothelial cell proliferation. *Biomaterials* 2004;25:1883–90.
- [229] Li M, Mondrinos MJ, Gandhi MR, Ko FK, Weiss AS, Leikis PI. Electrospun protein fibers as matrices for tissue engineering. *Biomaterials* 2005;26:5999–6008.
- [230] Li WJ, Tuli R, Huang X, Laquerriere P, Tuan RS. Multilineage differentiation of human mesenchymal stem cells in a three-dimensional nanofibrous scaffold. *Biomaterials* 2005;26:5158–66.
- [231] Dvir T, Timko BP, Kohane DS, Langer R. Nanotechnological strategies for engineering complex tissues. *Nat Nanotechnol* 2011;6:13–22.
- [232] Unnithan AR, Barakat NAM, Pichiah PBT, Gnanasekaran G, Nirmala R, Cha YS, et al. Wound-dressing materials with antibacterial activity from electrospun polyurethane-dextran nanofiber mats containing ciprofloxacin HCl. *Carbohydr Polym* 2012;90:1786–93.
- [233] Abdeljawad AM, Hudson SM, Rojas OJ. Antimicrobial wound dressing nanofiber mats from multicomponent (chitosan/silver-NPs/polyvinyl alcohol) systems. *Carbohydr Polym* 2014;100:166–78.
- [234] Burger C, Hsiao BS, Chu B. Nanofibrous materials and their applications. *Annu Rev Mater Res* 2006;36:333–68.
- [235] Yang Y, Xia T, Zhi W, Wei L, Weng J, Zhang C, et al. Promotion of skin regeneration in diabetic rats by electrospun core-sheath fibers loaded with basic fibroblast growth factor. *Biomaterials* 2011;32:4243–54.
- [236] Xie J, Macewen MR, Ray WZ, Liu W, Siewe DY, Xia Y. Radially aligned, electrospun nanofibers as dural substitutes for wound closure and tissue regeneration applications. *ACS Nano* 2010;4:5027–36.
- [237] Angeles M, Cheng HL, Velankar SS. Emulsion electrospinning: composite fibers from drop breakup during electrospinning. *Polym Adv Technol* 2010;19:728–33.
- [238] Tian Y, Wang H, Liu Y, Mao L, Chen W, Zhu Z, et al. A peptide-based nanofibrous hydrogel as a promising DNA nanovector for optimizing the efficacy of HIV vaccine. *Nano Lett* 2014;14:1439–45.
- [239] Kalate BM, Behbahani M, Mashhadizadeh MH, Bagheri A, Hosseini Davarani SS, Farahani A. Mercapto-ordered carbohydrate-derived porous carbon electrode as a novel electrochemical sensor for simple and sensitive ultra-trace detection of omeprazole in biological samples. *Mat Sci Eng C* 2015;48:213–9.
- [240] Martin JT, Milby AH, Ikuta K, Poudel S, Pfeifer CG, Elliott DM, et al. A radiopaque electrospun scaffold for engineering fibrous musculoskeletal tissues: scaffold characterization and in vivo applications. *Acta Biomater* 2015;26:97–104.
- [241] Ding B, Wang M, Wang X, Yu J, Sun G. Electrospun nanomaterials for ultrasensitive sensors. *Mater Today* 2010;13:16–27.
- [242] Graffarend D, Heffels KH, Beer MV, Gasteier P, Möller M, Boehm G, et al. Degradable polyester scaffolds with controlled surface chemistry combining minimal protein adsorption with specific bioactivation. *Nat Mater* 2011;10:67–73.
- [243] Marklein RA, Burdick JA. Controlling stem cell fate with material design. *Adv Mater* 2010;22:175–89.
- [244] Kim B, Lopez-Ferrer D, Lee SM, Ahn H, Nair S, Kim S, et al. Highly stable trypsin-aggregate coatings on polymer nanofibers for repeated protein digestion. *Proteomics* 2009;9:1893–900.
- [245] Lee B, Kim BC, Chang MS, Han SK, Na HB, Yong IP, et al. Efficient protein digestion using highly-stable and reproducible trypsin coatings on magnetic nanofibers. *Chem Eng J* 2016;288:770–7.
- [246] Moore AN, Hartgerink JD. Self-assembling multidomain peptide nanofibers for delivery of bioactive molecules and tissue regeneration. *Acc Chem Res* 2017;50:714–22.
- [247] Maleki M, Natalello A, Pugliese R, Gelain F. Fabrication of nanofibrous electrospun scaffolds from a heterogeneous library of co- and self-assembling peptides. *Acta Biomater* 2017;51:268–78.
- [248] Qian Y, Chen H, Yang X, Yang J, Zhou X, Zhang F, et al. The preosteoblast response of electrospinning PLGA/PCL nanofibers: effects of biomimetic architecture and collagen I. *Int J Nanomed Nanosurg* 2016;11:4157–71.
- [249] Niu X, Liu Z, Feng T, Chen S, Lei L, Jiang T, et al. Sustained delivery of calcium and orthophosphate ions from amorphous calcium phosphate and poly(L-lactic acid)-based electrospinning nanofibrous scaffold. *Sci Rep* 2017;7, 45655/1–9.
- [250] Lakshmanan R, Kumaraswamy P, Krishnan UM, Sethuraman S. Engineering a growth factor embedded nanofiber matrix niche to promote vascularization for functional cardiac regeneration. *Biomaterials* 2016;97:176–95.
- [251] Hanssen AD, Spanghel MJ. Practical applications of antibiotic-loaded bone cement for treatment of infected joint replacements. *Clin Orthop Relat Res* 2004;427:79–85.
- [252] Sanna V, Nurra S, Pala N, Marceddu S, Pathania D, Neamati N, et al. Targeted nanoparticles for the delivery of novel bioactive molecules to pancreatic Cancer cells. *J Med Chem* 2016;59:5209–20.
- [253] Koh A, Carpenter AW, Slomberg DL, Schoenfisch MH. Nitric oxide-releasing silica nanoparticle-doped polyurethane electrospun fibers. *ACS Appl Mater Interfaces* 2013;5:7956–64.
- [254] Dai X, Li Z, Lai M, Shu S, Du Y, Zhou ZH, et al. In situ structures of the genome and genome-delivery apparatus in a single-stranded RNA virus. *Nature* 2017;541:112–6.
- [255] Matthew RA, Gopi MM, Menon P, Jayakumar R, Vijayachandran LS. Synthesis of electrospun silica nanofibers for protein/DNA binding. *Mater Lett* 2016;184:5–8.
- [256] Pine SR, Ryan BM, Varticovski L, Robles AI, Harris CC. Microenvironmental modulation of asymmetric cell division in human lung cancer cells. *Proc Natl Acad Sci USA* 2010;107:2195–200.
- [257] Lutolf MP, Hubbell JA. Synthetic biomaterials as instructive extracellular microenvironments for morphogenesis in tissue engineering. *Nat Biotechnol* 2005;23:47–55.
- [258] Lin F, Yu J, Tang W, Zheng J, Xie S, Becker ML. Postelectrospinning “Click” modification of degradable amino acid-based poly(ester urea) nanofibers. *Macromolecules* 2013;46:9515–25.
- [259] Barnes CP, Sell SA, Boland ED, Simpson DG, Bowlin GL. Nanofiber technology: designing the next generation of tissue engineering scaffolds. *Adv Drug Del Rev* 2007;59:1413–33.
- [260] Capulli AK, Macqueen LA, Sheehy SP, Parker KK. Fibrous scaffolds for building hearts and heart parts. *Adv Drug Del Rev* 2016;96:83–102.
- [261] Sell SA, McClure MJ, Garg K, Wolfe PS, Bowlin GL. Electrospinning of collagen/biopolymers for regenerative medicine and cardiovascular tissue engineering. *Adv Drug Del Rev* 2009;61:1007–19.
- [262] Duan B, Yuan WX. Hybrid nanofibrous membranes of PLGA/chitosan fabricated via an electrospinning array. *J Biomed Mater Res A* 2007;83:868–78.
- [263] Groeber F, Holeiter M, Hampel M, Hinderer S, Schenkelyland K. Skin tissue engineering—in vivo and in vitro applications. *Clin Plast Surg* 2012;39:33–58.
- [264] Liu W, Thomopoulos S, Xia Y. Electrospun nanofibers for regenerative medicine. *Adv Healthc Mater* 2012;1:10–25.
- [265] Saracino GA, Cignogni D, Silva D, Caprini A, Gelain F. Nanomaterials design and tests for neural tissue engineering. *Chem Soc Rev* 2013;42:225–62.
- [266] Kang YG, Shin JW, Park SH, Kim YM, Gu SR, Wu Y, et al. A three-dimensional hierarchical scaffold fabricated by a combined rapid prototyping technique and electrospinning process to expand hematopoietic stem/progenitor cells. *Biotechnol Lett* 2016;38:175–817.
- [267] Morelli S, Salerno S, Piscioneri A, Papenburg Bj, Di VA Giusi G, Canonaco M, et al. Influence of micro-patterned PLLA membranes on outgrowth and orientation of hippocampal neurites. *Biomaterials* 2010;31:7000–11.
- [268] Baker BM, Britta T, Wang WY, Sakar MS, Kim IL, Shenoy VB, et al. Cell-mediated fiber recruitment drives extracellular matrix mechanosensing in engineered fibrillar microenvironments. *Nat Mater* 2015;14:1262–8.
- [269] Yang F, Murugan R, Wang S, Ramakrishna S. Electrospinning of nano/micro scale poly(L-lactic acid) aligned fibers and their potential in neural tissue engineering. *Biomaterials* 2005;26:2603–10.
- [270] Xie J, Macewen MR, Li X, Sakiyama-Elbert SE, Xia Y. Neurite outgrowth on nanofiber scaffolds with different orders, structures, and surface properties. *ACS Nano* 2009;3:1151–9.
- [271] Surrao DC, Waldman SD, Amsden BG. Biomimetic poly(lactide) based fibrous scaffolds for ligament tissue engineering. *Acta Biomater* 2012;8:3997–4006.
- [272] Zhang C, Gao C, Chang MW, Ahmad Z, Li JS. Continuous micron-scaled rope engineering using a rotating multi-nozzle electrospinning emitter. *Appl Phys Lett* 2016;109, 151903/1–4.
- [273] John J, Nair SV, Deepthy M. Integrating substrateless electrospinning with textile technology for creating biodegradable three-dimensional structures. *Nano Lett* 2015;15:5420–6.
- [274] Chang G, Shen J. Fabrication of Microropes via Bi-electrospinning with a rotating needle collector. *Macromol Rapid Commun* 2010;31:2151–4.
- [275] Cheng S, Jin Y, Wang N, Cao F, Zhang W, Bai W, et al. Self-adjusting, polymeric multilayered roll that can keep the shapes of the blood vessel scaffolds during biodegradation. *Adv Mater* 2017;29, 1700171/1–8.

- [276] Buitrago JO, Patel KD, El-Fiqi A, Lee JH, Kundu B, Lee HH, et al. Silk fibroin/collagen protein hybrid cell-encapsulating hydrogels with tunable gelation and improved physical and biological properties. *Acta Biomater* 2018;69:218–33.
- [277] Song W, An D, Kao DI, Lu YC, Dai G, Chen S, et al. Nanofibrous microposts and microwells of controlled shapes and their hybridization with hydrogels for cell encapsulation. *ACS Appl Mater Interfaces* 2014;6:7038–44.
- [278] An D, Ji Y, Chiu A, Lu YC, Song W, Zhai L, et al. Developing robust, hydrogel-based, nanofiber-enabled encapsulation devices (NEEDs) for cell therapies. *Biomaterials* 2015;37:40–8.
- [279] Hettiaratchy S, Dziewulski P. ABC of burns. Introduction. *BMJ* 2004;328:1366–8.
- [280] Torpy JM, Lynn C, Glass RM. JAMA patient page. Burn injuries. *J Am Med Assoc* 2009;302:1828.
- [281] Rieger KA. Designing electrospun nanofiber mats to promote wound healing – a review. *J Mater Chem B Mater Biol Med* 2013;1:4531–41.
- [282] Lalani R, Liu L. Electrospun zwitterionic poly(sulfobetaine methacrylate) for nonadherent, superabsorbent, and antimicrobial wound dressing applications. *Biomacromolecules* 2012;13:1853–63.
- [283] Li CW, Wang Q, Li J, Hu M, Shi SJ, Li ZW, et al. Silver nanoparticles/chitosan oligosaccharide/poly(vinyl alcohol) nanofiber promotes wound healing by activating TGF $\beta$ 1/Smad signaling pathway. *Int J Nanomed Nanosurg* 2015;11:373–86.
- [284] Ganeshkumar M, Ponrasu T, Krithika R, Iyappan K, Gayathri VS, Suguna L. Topical application of Acalypha indica accelerates rat cutaneous wound healing by up-regulating the expression of Type I and III collagen. *J Ethnopharmacol* 2012;142:14–22.
- [285] Verrecchia F, Mauviel A. Control of connective tissue gene expression by TGF $\beta$ : role of smad proteins in fibrosis. *Curr Rheumatol Rep* 2002;4:143–9.
- [286] Xin Z, Sun X, Yildirimler L, Qi L, Zhi YL, Zheng R, et al. Cell infiltrative hydrogel fibrous scaffolds for accelerated wound healing. *Acta Biomater* 2016;49:66–77.
- [287] Jiang K, Long YZ, Chen ZJ, Liu SL, Huang YY, Jiang X, et al. Airflow-directed *in situ* electrospinning of a medical glue of cyanoacrylate for rapid hemostasis in liver resection. *Nanoscale* 2014;6:7792–8.
- [288] Dai X, Liu J, Zheng H, Wichmann J, Hopfner U, Sudhop S, et al. Nano-formulated curcumin accelerates acute wound healing through Dkk-1-mediated fibroblast mobilization and MCP-1-mediated anti-inflammation. *NPG Asia Mater* 2017;9, e368/1–14.
- [289] Xin Z, He W, Zhang J, Li X, Wu Y, Wei Y, et al. Functional poly( $\epsilon$ -caprolactone)/chitosan dressings with nitric oxide-releasing property improve wound healing. *Acta Biomater* 2017;54:128–37.
- [290] Kitsara M, Agbulut O, Kontziamasis D, Chen Y, Menasché P. Fibers for hearts: a critical review on electrospinning for cardiac tissue engineering. *Acta Biomater* 2016;48:20–40.
- [291] Xiao J, Chen S, Yi J, Zhang HF, Ameer GA. A Cooperative Copper Metal-Organic Framework-Hydrogel System Improves Wound Healing in Diabetes. *Adv Funct Mater* 2016;27, 1604872/1–10.
- [292] Bhang SH, Jang WS, Han J, Yoon JK, La WG Lee E, Kim YS, et al. Zinc oxide nanorod-based piezoelectric dermal patch for wound healing. *Adv Funct Mater* 2017;27, 1603497/1–13.
- [293] Mayuri PV, Ramesh P. Fabrication and characterization of silver nanoparticle impregnated uniaxially aligned fibre yarns by one-step electrospinning process. *J Mater Sci* 2016;51:2739–46.
- [294] Paten JA, Siadat SM, Susilo ME, Ismail EN, Stoner JL, Rothstein JP, et al. Flow-induced crystallization of collagen: a potentially critical mechanism in early tissue formation. *ACS Nano* 2016;10:5027–40.
- [295] Coneski PN, Nash JA, Schoenfisch MH. Nitric oxide-releasing electrospun polymer microfibers. *ACS Appl Mater Interfaces* 2011;3:426–32.
- [296] Song DW, Kim SH, Kim HH, Lee KH, Ki CS, Park YH. Multi-biofunction of antimicrobial peptide-immobilized silk fibroin nanofiber membrane: implications for wound healing. *Acta Biomater* 2016;39:146–55.
- [297] Kandhasamy S, Perumal S, Madhan B, Umamaheswari N, Banday JA, Perumal PT. Synthesis and fabrication of collagen coated osthiamide electrospun nanofiber scaffold for wound healing. *ACS Appl Mater Interfaces* 2017;9:8556–68.
- [298] Ali IH, Khalil IA, El-Sherbiny IM. Single-dose electrospun nanoparticles-in-Nanofibers wound dressings with enhanced epithelialization, collagen deposition, and granulation properties. *ACS Appl Mater Interfaces* 2016;8:14453–69.
- [299] Patra HK, Sharma Y, Islam MM, Jafari MJ, Murugan NA, Kobayashi H, et al. Inflammation-sensitive *in situ* smart scaffolding for regenerative medicine. *Nanoscale* 2016;8:17213–22.
- [300] Nie H, Wang CH. Fabrication and characterization of PLGA/HAp composite scaffolds for delivery of BMP-2 plasmid DNA. *J Control Release* 2007;120:111–21.
- [301] Hwang TH, Jung DS, Kim JS, Kim BG, Choi JW. One-dimensional carbon-sulfur composite fibers for Na-S rechargeable batteries operating at room temperature. *Nano Lett* 2013;13:4532–8.
- [302] Wang Y, Qiao W, Wang B, Zhang Y, Shao P, Yin T. Electrospun composite nanofibers containing nanoparticles for the programmable release of dual drugs. *Polym J* 2011;43:478–83.
- [303] Yang Y, Yang Q, Fang Z, Zhao Y, Jia X, Yuan X, et al. Electrospun PELCL membranes loaded with QK peptide for enhancement of vascular endothelial cell growth. *J Mater Sci Mater Med* 2016;27, 106/1–10.
- [304] Mickova A, Buzgo M, Benada O, Rampichova M, Fisar Z, Filova E, et al. Core/shell nanofibers with embedded liposomes as a drug delivery system. *Biomacromolecules* 2012;13:952–62.
- [305] Yohe ST, Colson YL, Grinstaff MW. Superhydrophobic materials for tunable drug release: using displacement of air to control delivery rates. *J Am Chem Soc* 2012;134:2016–9.
- [306] Song B. Ultrasound-triggered dual-drug release from poly(lactic-co-glycolic acid)/mesoporous silica nanoparticles electrospun composite fibers. *Regen Biomater* 2015;5:229–37.
- [307] Liu D, Liu S, Jing X, Li X, Li W, Huang Y. Necrosis of cervical carcinoma by dichloroacetate released from electrospun polylactide mats. *Biomaterials* 2012;33:4362–9.
- [308] Rujitanaroj PO, Jao B, Yang J, Wang F, Anderson JM, Wang J, et al. Controlling fibrous capsule formation through long-term down-regulation of collagen type I (COL1A1) expression by nanofiber-mediated siRNA gene silencing. *Acta Biomater* 2013;9:4513–24.
- [309] Cho K, Lee HJ, Han SW, Min JH, Park H, Koh WG. Multi-compartmental hydrogel microparticles fabricated by combination of sequential electrospinning and photopatterning. *Angew Chem Int Ed* 2015;54:11511–5.
- [310] Huang ZM, He CL, Yang A, Zhang Y, Han XJ, Yin J, et al. Encapsulating drugs in biodegradable ultrafine fibers through co-axial electrospinning. *J Biomed Mater Res A* 2006;77:169–79.
- [311] Honarbakhsh S, Pourdeyhimi B. Scaffolds for drug delivery, part I: electrospun porous poly(lactic acid) and poly(lactic acid)/poly(ethylene oxide) hybrid scaffolds. *J Mater Sci* 2011;46:2874–81.
- [312] Na S, Min L, Wang J, Wang Z, Li X, Jiang B, et al. Chitosan nanofibers for specific capture and nondestructive release of CTCs assisted by pCBMA brushes. *Small* 2016;12:5090–7.
- [313] Gilchrist SE, Lange D, Letchford K, Bach H, Fazli L, Burt HM. Fusidic acid and rifampicin co-loaded PLGA nanofibers for the prevention of orthopedic implant associated infections. *J Control Release* 2013;170:64–73.
- [314] Wang C, Wang M. Electrospun Multicomponent and Multifunctional Nanofibrous Bone Tissue Engineering Scaffolds. *J Mater Chem B Mater Biol Med* 2017;5:1388–99.
- [315] Nabzdyk CS, Chun MC, Oliverallen HS, Pathan SG, Phaneuf MD, You JO, et al. Gene silencing in human aortic smooth muscle cells induced by PEI-siRNA complexes released from dip-coated electrospun poly(ethylene terephthalate) grafts. *Biomaterials* 2014;35:3071–9.
- [316] Wei CL, Rujitanaroj PO, Lee DK, Messersmith PB, Stanton LW, Goh E, et al. Nanofibrous scaffold-mediated REST knockdown to enhance neuronal differentiation of stem cells. *Biomaterials* 2013;34:3581–90.
- [317] Shi D. Integrated multifunctional nanosystems for medical diagnosis and treatment. *Adv Funct Mater* 2010;19:3356–73.
- [318] Schneider D, Rabe T, Riedl T, Dobbertin T, Kröger M, Becker E, et al. An ultraviolet organic thin-film solid-state laser for biomarker applications. *Adv Mater* 2005;17:31–4.
- [319] Cong Y, Xu M, Frantisek S, Fréchet JMJ. Preparation of monolithic polymers with controlled porous properties for microfluidic chip applications using photoinitiated free-radical polymerization. *J Polym Sci Part A: Polym Chem* 2002;40:755–69.
- [320] Serafim BM, Leitolis A, Crestani S, Marcon BH, Foti L, Petzhold CL, et al. Electrospinning induced surface activation (EISA) of highly porous PMMA microfiber mats for HIV diagnostic. *J Mater Chem B Mater Biol Med* 2016;4:6004–11.
- [321] Wang H, Wang D, Peng Z, Tang W, Li N, Liu F. Assembly of DNA-functionalized gold nanoparticles on electrospun nanofibers as a fluorescent sensor for nucleic acids. *Chem Commun (Camb)* 2013;49:5568–70.
- [322] Ma L, Yang G, Wang N, Zhang P, Guo F, Meng J, et al. Trap effect of three-dimensional fibers network for high efficient cancer-cell capture. *Adv Healthc Mater* 2015;4:838–43.
- [323] Long Y, Zhou C, Wang C, Cai H, Yin C, Yang Q, et al. Ultrasensitive visual detection of HIV DNA biomarkers via a multi-amplification nanoplatform. *Sci Rep* 2016;6, 23949/1–11.
- [324] Yang D, Niu X, Liu Y, Wang Y, Gu X, Song L, et al. Electrospun nanofibrous membranes: a novel solid substrate for microfluidic immunoassays for HIV. *Adv Mater* 2008;20:4770–5.
- [325] Chen C, Chen J, Wang T, Liu M. Fabrication of helical nanoribbon polydiacetylene via supramolecular gelation: circularly polarized luminescence and novel diagnostic chiroptical signals for sensing. *ACS Appl Mater Interfaces* 2016;8:30608–15.
- [326] Wang H, Tang W, Wei H, Zhao Y, Hu S, Guan Y, et al. Integrating dye-intercalated DNA dendrimers with electrospun nanofibers: a new fluorescent sensing platform for nucleic acids, proteins, and cells. *J Mater Chem B Mater Biol Med* 2015;3:3541–7.
- [327] Liu Y, Yang D, Yu T, Jiang X. Incorporation of electrospun nanofibrous PVDF membranes into a microfluidic chip assembled by PDMS and scotch tape for immunoassays. *Electrophoresis* 2009;30:3269–75.
- [328] Tseng H, Lee AW, Wei P, Chang Y, Chen J. Clinical diagnosis of colorectal Cancer Using electrospun triple-blend fibrous mat-based capture assay of circulating tumor cells. *J Mater Chem B Mater Biol Med* 2016;4:6565–80.
- [329] Aguado BA, Caffe JR, Nanavati D, Rao SS, Bushnell GG, Azarin SM, et al. Extracellular matrix mediators of metastatic cell colonization characterized using scaffold mimics of the pre-metastatic niche. *Acta Biomater* 2016;33:13–24.

- [330] Jang JS, Choi SJ, Kim SJ, Hakim M, Kim ID. Rational design of highly porous SnO<sub>2</sub> nanotubes functionalized with biomimetic nanocatalysts for direct observation of simulated diabetes. *Adv Funct Mater* 2016;26:4740–8.
- [331] Zheng Y, Bai H, Huang Z, Tian X, Nie FQ, Zhao Y, et al. Directional water collection on wetted spider silk. *Nature* 2010;463:640–3.
- [332] Lee H, Lee BP, Messersmith PB. A reversible wet/dry adhesive inspired by mussels and geckos. *Nature* 2007;448:338–41.
- [333] Barthlott W, Neinhuis C. Purity of the sacred lotus, or escape from contamination in biological surfaces. *Planta* 1997;202:1–8.
- [334] Srinivasarao M. Nano-optics in the biological world: beetles, butterflies, birds, and moths. *Chem Rev* 1999;99:1935–61.
- [335] And SW, Wagner HD. The material bone: structure-mechanical function relations. *Annu Rev Mater Res* 1998;28:271–98.
- [336] Ke P, Jiao XN, Ge XH, Xiao WM, Yu B. From macro to micro: structural biomimetic materials by electrospinning. *RSC Adv* 2014;4:39704–24.
- [337] Vincent JV, Bogatyrev OA, Bogatyrev NR, Bowyer A, Pahl AK. Biomimetics: its practice and theory. *J R Soc Interface* 2006;3:471–82.
- [338] Sarikaya M, Tamerler C, Jen AK, Schulten K, Baneyx F. Molecular biomimetics: nanotechnology through biology. *Nat Mater* 2003;2:577–85.
- [339] Nakanishi T, Michinobu T, Yoshida K, Shirahata N, Ariga K, Möhwald H, et al. Nanocarbon superhydrophobic surfaces created from fullerene-based hierarchical supramolecular assemblies. *Adv Mater* 2008;20:443–6.
- [340] Yue B, Zhang B, You J, Li Y, Li L, Li J. Lotus-effect" tape: imparting superhydrophobicity to solid materials with an electrospun Janus composite mat. *RSC Adv* 2016;6:17215–21.
- [341] Zhang X, Shi F, Niu J, Jiang Y, Wang Z. Superhydrophobic surfaces: from structural control to functional application. *J Mater Chem* 2008;18:621–33.
- [342] Zhang M, Atkinson KR, Baughman RH. Multifunctional carbon nanotube yarns by downsizing an ancient technology. *Science* 2004;306:1358–61.
- [343] Dong H, Wang N, Wang L, Bai H, Wu J, Zheng Y, et al. Bioinspired electrospun knotted microfibers for fog harvesting. *ChemPhysChem* 2012;13:1153–6.
- [344] Miyauchi Y, Ding B, Shiratori S. Fabrication of a silver-ragwort-leaf-like super-hydrophobic micro/nanoporous fibrous mat surface by electrospinning. *Nanotechnology* 2006;17:5151–6.
- [345] Jiang L, Zhao Y, Zhai J. A lotus-leaf-like superhydrophobic surface: a porous Microsphere/Nanofiber composite film prepared by electrohydrodynamics. *Angew Chem Int Ed* 2004;43:4338–41.
- [346] Yao S, Liu X, Yu S, Wang X, Zhang S, Wu Q, et al. Co-effects of matrix low elasticity and aligned topography on stem cell neurogenic differentiation and rapid neurite outgrowth. *Nanoscale* 2016;8:10252–65.
- [347] Zhao Y, Miao X, Lin J, Li X, Bian F, Wang J, et al. Coiled plant tendril bioinspired fabrication of helical porous microfibers for crude oil cleanup. *Global Chall* 2017;1, 1600021/1–6.
- [348] Tian X, Bai H, Zheng Y, Jiang L. Drug delivery: bio-inspired heterostructured bead-on-String fibers that respond to environmental wetting. *Adv Funct Mater* 2011;21:1330.
- [349] Xiang G, Song J, Ping J, Zhang X, Li X, Xiao X, et al. Polydopamine-templated hydroxyapatite reinforced polycaprolactone composite nanofibers with enhanced cytocompatibility and osteogenesis for bone tissue engineering. *ACS Appl Mater Interfaces* 2016;8:3499–515.
- [350] Wade RJ, Bassin EJ, Rodell CB, Burdick JA. Protease-degradable electrospun fibrous hydrogels. *Nat Commun* 2015;6:6639.